



RESEARCH ARTICLE

10.1029/2018TC005018

Key Points:

- Geochronological and structural evidence suggest close temporal and spatial relationship between basement grain and younger rift structure
- Rapid establishment of rift length (within 4–20% of rift life) suggests “constant-length model” for fault growth may apply also at rift scale
- Tip propagation, relay breaching, and linkage may, however, dominate border fault systems during early rapid lengthening

Correspondence to:

A. Rotevatn,
atle.rotevatn@uib.no

Citation:

Rotevatn, A., Kristensen, T. B., Ksienzyk, A. K., Wemmer, K., Henstra, G. A., Midtkandal, I., Grundvåg, S.-A., & Andresen, A. (2018). Structural inheritance and rapid rift-length establishment in a multiphase rift: The East Greenland rift system and its Caledonian orogenic ancestry. *Tectonics*, 37, 1858–1875. <https://doi.org/10.1029/2018TC005018>

Received 6 FEB 2018

Accepted 7 MAY 2018




Accepted article online 21 MAY 2018

Published online 17 JUN 2018

©2018. The Authors.

This is an open access article under the terms of the Creative Commons Attribution-NonCommercial-NoDerivs License, which permits use and distribution in any medium, provided the original work is properly cited, the use is non-commercial and no modifications or adaptations are made.

Structural Inheritance and Rapid Rift-Length Establishment in a Multiphase Rift: The East Greenland Rift System and its Caledonian Orogenic Ancestry

A. Rotevatn¹ , T. B. Kristensen¹, A. K. Ksienzyk¹, K. Wemmer², G. A. Henstra¹, I. Midtkandal³ , S.-A. Grundvåg^{4,5}, and A. Andresen³ 

¹Department of Earth Science, University of Bergen, Bergen, Norway, ²Geowissenschaftliches Zentrum der Georg-August Universität, Göttingen, Germany, ³Department of Geosciences, University of Oslo, Oslo, Norway, ⁴Department of Arctic Geology, University Centre in Svalbard, Svalbard, Norway, ⁵Now at Department of Geosciences, UiT The Arctic University of Norway, Tromsø, Norway

Abstract We investigate (i) margin-scale structural inheritance in rifts and (ii) the time scales of rift propagation and rift length establishment, using the East Greenland rift system (EGR) as an example. To investigate the controls of the underlying Caledonian structural grain on the development of the EGR, we juxtapose new age constraints on rift faulting with existing geochronological and structural evidence. Results from K-Ar illite fault dating and syn-rift growth strata in hangingwall basins suggest initial faulting in Mississippian times and episodes of fault activity in Middle-Late Pennsylvanian, Middle Permian, and Middle Jurassic to Early Cretaceous times. Several lines of evidence indicate a close relationship between low-angle late-to-post-Caledonian extensional shear zones (CESZs) and younger rift structure: (i) reorientation of rift fault strike to conform with CESZs, (ii) spatial coincidence of rift-scale transfer zones with CESZs, and (iii) close temporal coincidence between the latest activity (late Devonian) on the preexisting network of CESZs and the earliest rift faulting (latest Devonian to earliest Carboniferous). Late- to post-Caledonian extensional detachments therefore likely acted as a template for the establishment of the EGR. We also conclude that the EGR established its near-full length rapidly, i.e., within 4–20% of rift life. The “constant-length model” for normal fault growth may therefore be applicable at rift scale, but tip propagation, relay breaching, and linkage may dominate border fault systems during rapid lengthening.

1. Introduction

During continental rifting, the existence of an older, preexisting structural grain may profoundly affect the localization, growth, segmentation, and overall geometry of subsequent rift-related faults and basins. This has been shown in field and subsurface (seismic-based) studies (e.g., Duffy et al., 2015; Ebinger et al., 1997; Gibson et al., 2013; Henstra et al., 2015; Milani & Davison, 1988; Miller et al., 2002; Moustafa, 1997; Salomon et al., 2015; Theunissen et al., 1996; Whipp et al., 2014) as well as in physical and numerical modeling experiments (e.g., Autin et al., 2013; Bonini et al., 1997; Brune et al., 2017; Corti et al., 2007; Michon & Sokoutis, 2005; Tommasi & Vauchez, 2001). In particular, the presence of a preexisting *orogenic* structural grain can play an important role in the evolution of rift basins worldwide (Coward, 1990; Vauchez et al., 1997). One of the most prominent examples is the Scandinavian Caledonides, whose structural imprint has profoundly affected structural development during Paleozoic to Cenozoic rifting and passive margin formation (e.g., Christiansson et al., 2000; Færseth et al., 1995; Fossen et al., 2017; Gudlaugsson et al., 1998; Henstra et al., 2015; Odinsen et al., 2000; Osmundsen et al., 2002; Phillips et al., 2016; Tomasso et al., 2008). The rift basins of Scandinavia are located offshore (with the notable exception of the Carboniferous-Permian Oslo Graben; see e.g., Fossen et al., 2017), where an abundance of seismic and wellbore data represent a powerful resource to compare the subsurface rift structure with the onshore (and offshore) Caledonian structural grain (e.g., Phillips et al., 2016). In contrast, on the conjugate East Greenland margin, the relationship between (i) the structural grain related to the Caledonian orogeny and (ii) the younger Paleozoic-Mesozoic rift structure is far less well understood. The reasons for this may be many, but for the onshore East Greenland rift basins, where seismic and wellbore data are generally not available, it is clear that a different, field-based approach is needed to address structural inheritance.

The primary goal of this study is to improve the understanding of structural inheritance in rifts, using the East Greenland rift system as an example. A secondary goal of the study is to investigate whether the “constant-length model” for fault growth (Nicol et al., 2005, 2017; Walsh et al., 2002, 2003), which suggests that faults attain their near-full lengths early in their slip histories, is valid also at rift scale. The constant-length model has been shown to accurately describe fault growth at the scale of individual faults and fault arrays (e.g., Giba et al., 2012; Jackson et al., 2017; Jackson & Rotevatn, 2013; Rotevatn et al., 2018), but has not previously been proven to be applicable to entire rift systems.

To address the above study goals, we combine new and existing data and observations as we (i) present new radiometric age constraints on fault activity from the East Greenland rift system; (ii) juxtapose our results with a wide review of existing geochronological and structural evidence from previous studies; and (iii) evaluate the temporal, spatial, and geometric coincidence between Caledonian-derived low-angle shear zones and the younger rift structure in East Greenland. In doing so, we aim to achieve better constraints on the timing and localization of extensional rift-related faulting in East Greenland and to elucidate the controls of the underlying Caledonian structural grain on the development of the East Greenland rift system in Paleozoic to Mesozoic times. Samples for K-Ar dating of illite in fault gouges were collected from the Dombjerg Fault in Wollaston Forland, East Greenland (Figure 1). The Dombjerg Fault forms part of the Clavering-Dombjerg-Thomsen Land Fault (CDTF) Zone, a regionally significant rift-bounding fault in the East Greenland rift system. Like many basin-bounding faults in rift basins, the Dombjerg Fault Zone has likely been active during at least two phases of extensional movement (e.g., Surlyk & Korstgård, 2013). The main rift phase in Middle Jurassic to Early Cretaceous times is well-documented by the presence of fault-ward expanding syn-rift deep-water clastics in the Wollaston Forland hangingwall basin (Henstra et al., 2016; Surlyk, 1978, 1984, 1991), whereas proposed earlier (Carboniferous-Permian?) phases of activity (Kristensen et al., 2016; Surlyk & Korstgård, 2013) have not been proven. By subjecting five fault gouge samples from the Dombjerg Fault Zone to K-Ar illite dating, in combination with rigorous review of previously published geochronological evidence, we can, for the first time, place specific age constraints on the timing and episodicity of rifting that caused slip to accumulate in the East Greenland rift system.

The results of this work have implications for understanding structural inheritance and the timescales of rift propagation globally, and may be applied to understand the structure and evolution of modern and ancient rift systems alike. The study is unique in that it investigates the influence of a preexisting structural grain on the evolution of an entire rift system (cf. Hayward & Ebinger, 1996), rather than individual faults and fault arrays (e.g., Keep & McClay, 1997); this has not been fully addressed before (e.g., Fossen et al., 2017; Smith & Mosley, 1993).

2. Geological Framework

The Paleozoic to Cenozoic geological history of East Greenland can be divided into four stages: (i) the poly-phased Ordovician to Devonian Caledonian orogeny (e.g., Higgins et al., 2008), involving both contraction and extension, including the development of several top-to-the east extensional detachments during late stages of contraction (e.g., Gee et al., 2008; Hartz et al., 2000; Higgins et al., 2008; Strachan, 1994); (ii) Devonian extension/transension with continued development of regionally significant extensional detachments (Augland et al., 2010) and “Old Red” basins (e.g., Andresen et al., 1998; Fossen, 2010; Gilotti & McClelland, 2008; Larsen & Bengaard, 1991); (iii) Late Paleozoic to Mesozoic rifting (e.g., Surlyk, 1990); and (iv) Paleocene-Eocene opening of the North Atlantic (e.g., Larsen & Watt, 1985; Mjelde et al., 2008).

2.1. The Caledonian Orogeny in East Greenland: A Tale of Contraction and Extension

The geology of East Greenland, and indeed the North Atlantic as a whole, is to a large degree dominated by the imprint of the Caledonian orogeny (e.g., Haller, 1971), which culminated during the continent-continent collision of Baltica and Laurentia in Late Silurian to Early Devonian times (Torsvik et al., 1996; Figure 2). In East Greenland, major Caledonian thrust sheets were emplaced as a result of top-to-the-west translation in (Ordovician to) Siluro-Devonian times, concurrent with the Ordovician to Early Devonian closure of the Late Proterozoic to Early Paleozoic Iapetus Ocean (Henriksen, 1985; Higgins et al., 2008; Strachan et al., 1994). The timing of Caledonian contraction in East Greenland is to some extent constrained; the earliest evidence interpreted to reflect Caledonian thrusting is a single Sensitive High-Resolution Ion Microprobe U-Pb zircon age at 445 Ma (Strachan et al., 1995), whereas the youngest published isotopic evidence

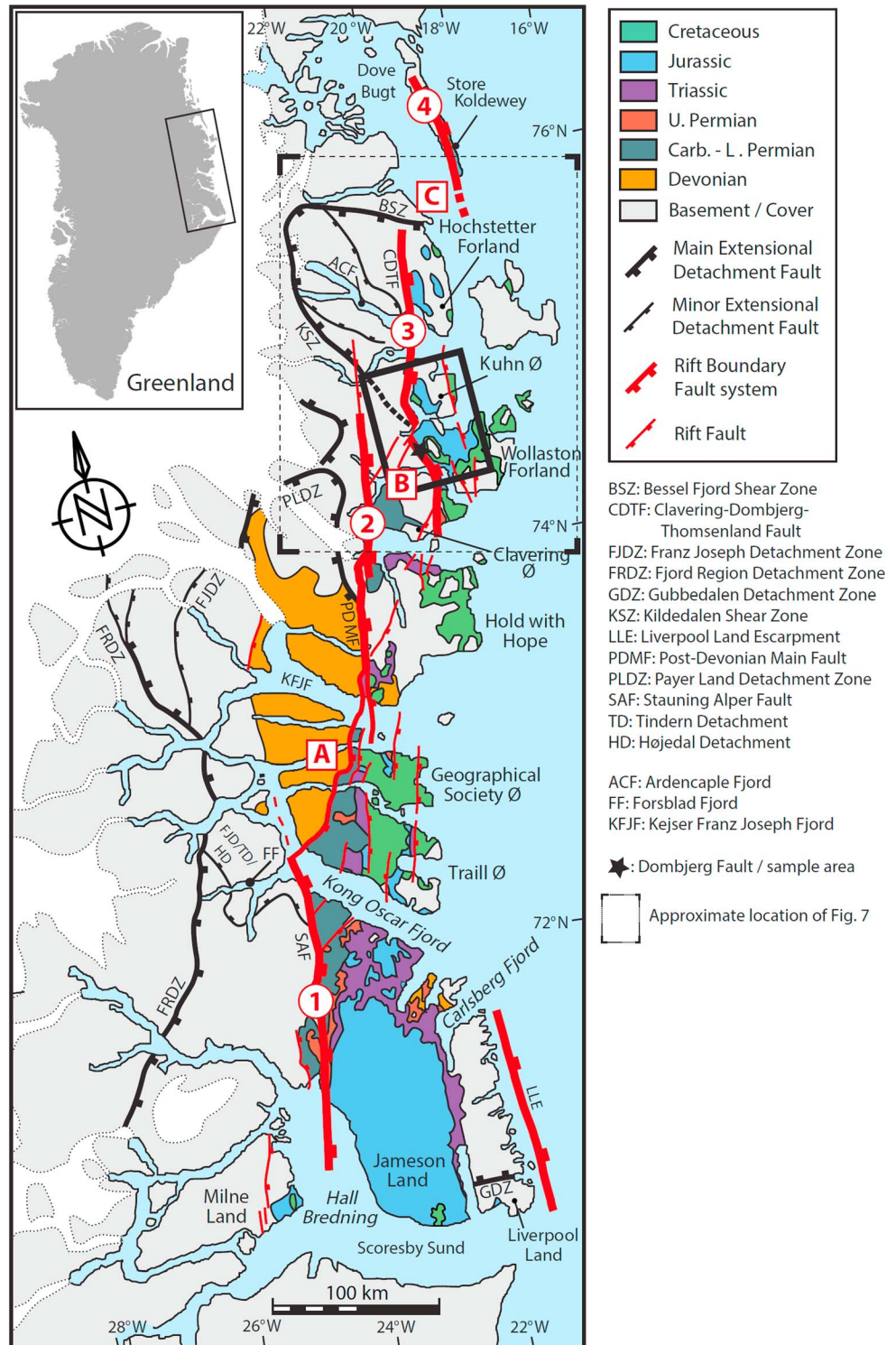


Figure 1. Regional geological map of the East Greenland Caledonides highlighting the Caledonian structural framework (structures marked with black line) and the East Greenland rift system (structures marked with red line). Note the proposed rift fault framework, comprising four first-order rift fault segments (numbered 1–4) separated by three first-order transfer zones (A through C). Location in East Greenland is shown on inset map. The locations of Figures 3 and 4 (bold black square) and Figure 7 (dotted black square) are indicated. Based on Henriksen (2003), Surlyk (2003), Andresen et al. (2007), and Henstra et al. (2016).

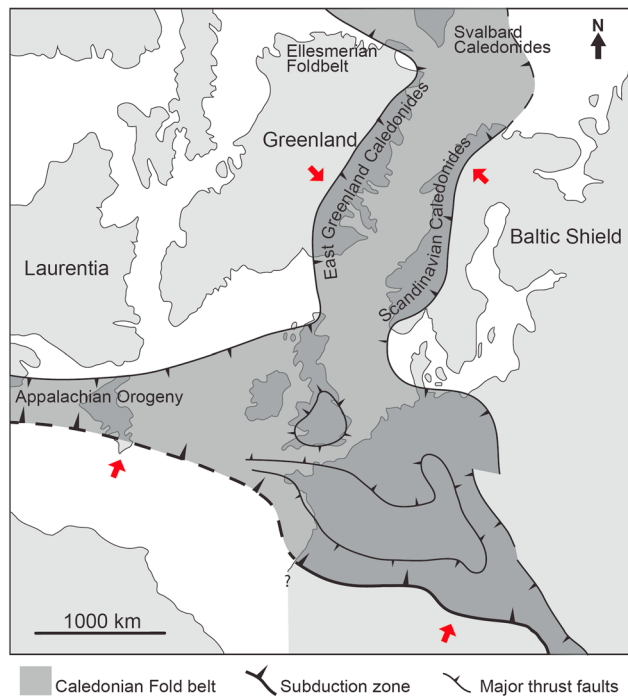


Figure 2. Paleogeographic map showing the areas affected by the Caledonian-Appalachian orogeny and the approximate configuration of today's landmasses at the time of continent-continent collision in Siluro-Devonian times. The red arrows represent schematic plate motion vectors. Based on Gee and Sturt (1985) and Cocks and Torsvik (2002).

interpreted to record thrusting is a U-Pb zircon age from the Dove Bugt area (Figure 1) at 404 Ma (Kalsbeek et al., 1993) and a muscovite Ar/Ar cooling age from the Caledonian foreland in Dronning Louise Land (west and inboard of Dove Bugt; see Figure 1) yielding 399 Ma (Dallmeyer et al., 1994).

During the late stages of the Caledonian orogeny, several top-to-the-east extensional shear zones developed in East Greenland. The most extensive of these is the N-trending, E-dipping Fjord Region Detachment Zone (FRDZ; Hartz & Andresen, 1995; Hartz et al., 2001; Andresen et al., 2007; Figure 1), a low-angle extensional detachment characterized by an up to 1-km-thick mylonite zone (Andresen et al., 1998). The FRDZ originated at more than 25 km depth and developed during progressively lower P-T conditions (Fossen, 2010; Gilotti & McClelland, 2008). At higher crustal levels, strain is largely localized in a 10–50 m wide, slightly steeper, brittle fault within the FRDZ (Andresen et al., 1998; Hartz & Andresen, 1995). A metamorphic break from greenschist- to amphibolite-facies across the shear zone suggests that it is associated with at least several tens of kilometers of extensional displacement (Fossen, 2010). Initially interpreted as a thrust, this regionally extensive extensional detachment was responsible for at least 25 km of vertical unroofing (Andresen et al., 1998). Isotopic evidence suggests that the FRDZ was active as an extensional detachment between 430 and 375 Ma, which means that the FRDZ accommodated both syn-contractual and postcontractual extension in the East Greenland Caledonides (Hartz et al., 2000).

The arcuate shear zone system comprised by the Kildedalen and Besselfjord Shear Zones (KSZ and BSZ; Dallmeyer et al., 1994; Friderichsen et al., 1994; Gilotti & McClelland, 2008) is of similar style and significance but is spatially restricted to a smaller area further north around Ardencape Fjord (Figure 1). Here the KSZ and BSZ form a scoop-shaped tract that separates Paleoproterozoic orthogneisses in the shear zone footwall from the Mesoproterozoic Smallefjord metasedimentary unit in the hangingwall (Dallmeyer et al., 1994; Friderichsen et al., 1994). The BSZ is an east to southeast-trending, moderately south to southwest-dipping, 150–200 m wide mylonite zone with down-to-the-SW extensional kinematic indicators (Friderichsen et al., 1994) and extends ~70–100 km from the area NW of Ardencape Fjord, to the eastern shores of Hochstetter Forland (Figure 1). The KSZ is characterized by a wide zone (1–3.5 km) of strongly tectonized amphibolite-facies mylonites with E-dipping foliations, showing down-to-the-E extensional kinematic indicators (Friderichsen et al., 1994). The KSZ is NW-striking and was initially mapped to a length of ~60 km S of Ardencape Fjord (e.g., Friderichsen et al., 1994; Figure 1); Friderichsen (1999) mapped its continuation to the SWE across Th. Thomsen Land for another 40 km (Figures 1, 3, and 4).

A series of normal faults rooted in the FRDZ developed in the hangingwall of the detachment. Several of these normal faults made it to the surface where they created deep Middle and Late Devonian basins and ridges (e.g., Gilotti & McClelland, 2008). Three distinct fault sets, striking N-S, NW-SW, and E-W, respectively, controlled the Middle and Late Devonian basins in the “Central Fjord Region” of Kong Oscar and Keiser Franz Joseph Fjords (Henriksen, 2003; Vischer, 1943; Figure 1). Similar steep normal faults developed above the KSZ and BSZ further to the north (Friderichsen et al., 1994; Figure 1).

2.2. From Devonian “Old Red” Basins to Protracted Rifting

In the Devonian, extension/transension led to the continued development of regionally significant extensional detachments (Augland et al., 2010) and “Old Red” basins (Andresen et al., 1998; Gilotti & McClelland, 2008; Larsen & Benggaard, 1991). More than 8 km of coarse-grained continental clastic deposits filled the Devonian “Old Red” Basin of the Central Fjord Region in East Greenland (Figure 1; Larsen & Benggaard, 1991; Larsen et al., 2008). Similar to other Devonian basins in the North Atlantic region, the basin formation is linked to the extensional collapse of the Caledonides (Fossen, 2010), although an influence of sinistral strike-slip faulting has been suggested (Larsen & Benggaard, 1991). Following Devonian extension,

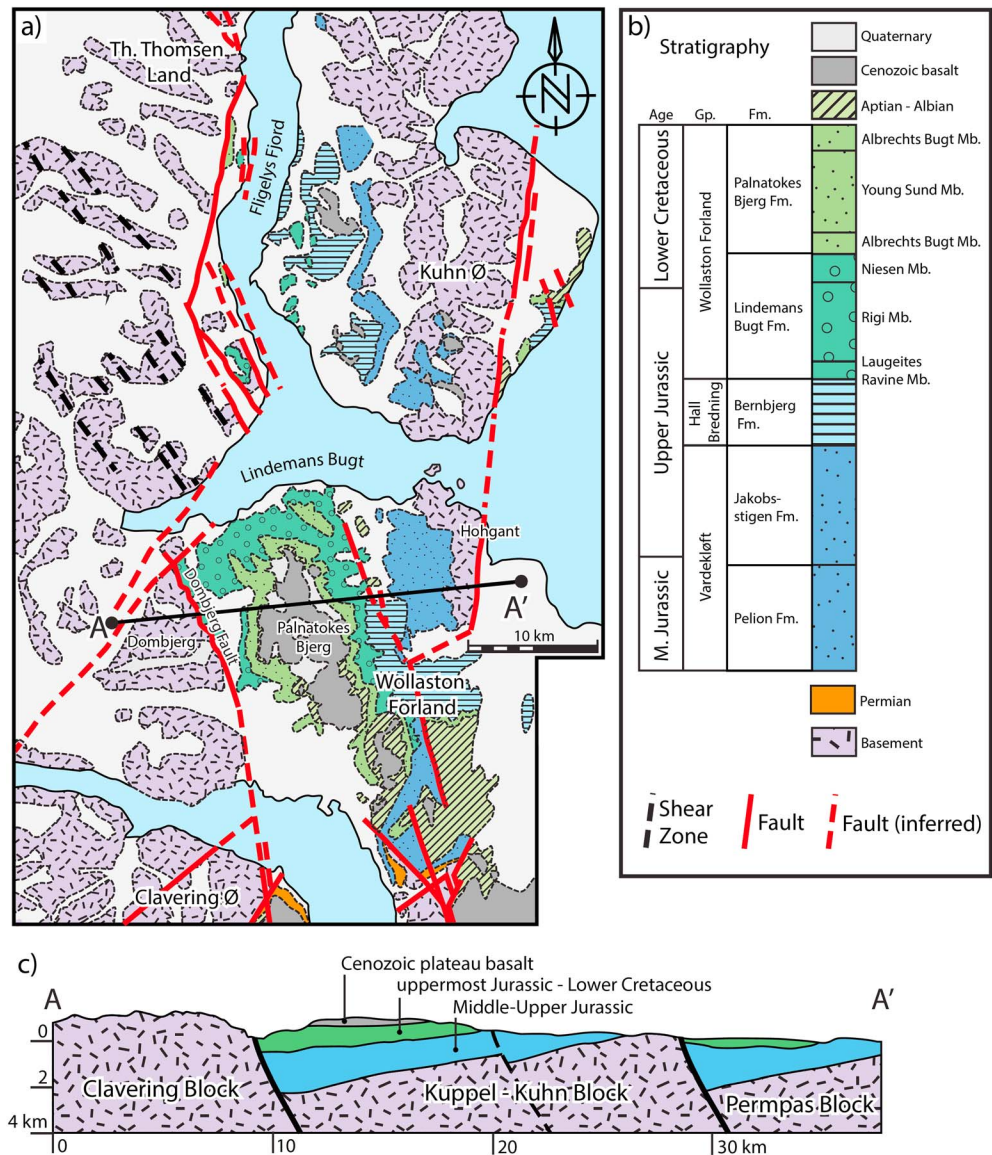


Figure 3. (top left) Geological map, (top right) stratigraphic column, and (bottom) geological cross section of the Wollaston Forland Basin. Surrounding areas are also shown. Location of the map is shown in Figure 1. The location of the profile A-A' (bottom) is shown on the map (top left). Based on Henriksen (2003), Surlyk (2003), and Henstra et al. (2016).

transension, and basin development, onset of E-W directed rifting in latest Devonian to Mississippian times marked the onset of a prolonged period of episodic rifting in Late Paleozoic to Mesozoic times (Surlyk, 1990). Most of the post-Devonian tectonic activity appears to have been localized to the area east of the Post-Devonian Main Fault (Figure 1). This can be seen already in Vischer's (1943) cross sections from the area between 74°N and 75°N, where dramatic thickness variations were observed across several of the faults, suggesting episodic fault activity in Late Paleozoic to Mesozoic times. During this time, key events recognized in the East Greenland rift system include (i) initial rifting in latest Devonian to Mississippian times (Stemmerik et al., 1991; Surlyk, 1990); (ii) rotational block faulting in Pennsylvanian to Early Permian times (Haller, 1971; Larsen, 1988; Surlyk, 1990; Surlyk et al., 1986); (iii) a Late Permian to earliest Triassic phase of relative tectonic quiescence and thermally driven subsidence (Larsen, 1988; Surlyk et al., 1986); (iv) renewed rifting and fault-controlled subsidence in the latest Early Triassic (Clemmensen, 1980; Seidler et al., 2004; Surlyk, 1990); (v) relative tectonic quiescence in Middle Triassic to Early Jurassic times (Surlyk, 1990); and (vi) a particularly well-documented phase of rifting in Middle Jurassic to earliest Cretaceous

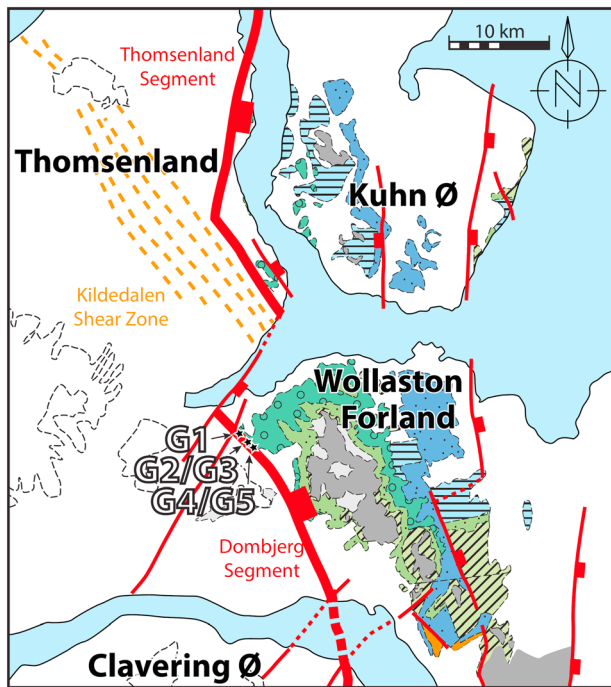


Figure 4. Schematic structural map showing the Dombjerg segment (i.e., the Dombjerg Fault) and the Thomsen Land segment of the Clavering-Dombjerg-Thomsen Land Fault system and its relationship with the SE-ward continuation of the Kildedalen Shear Zone. Sample locations for fault gouge samples G1 through G5 are indicated with black and yellow stars. Based on Henriksen (2003), Surlyk (2003), and Henstra et al. (2016).

times (Henstra et al., 2016; Maync, 1949; Surlyk, 1978; Surlyk & Korstgård, 2013; Vischer, 1943; Whitham et al., 1999). This protracted period of rifting culminated in the breakup of the North Atlantic in Paleocene-Eocene times (Larsen & Watt, 1985; e.g., Mjelde et al., 2008).

3. Structure of the East Greenland Rift System

The East Greenland rift system is characterized by a series of largely N-S trending, fault-bounded Paleozoic to Mesozoic basins found onshore and offshore East Greenland (Price et al., 1997; Surlyk, 1990). Onshore, a series of Carboniferous to Cretaceous basins occur in a 50–100 km wide belt along the eastern coastline of East Greenland between 68 and 77°N (Henriksen, 2003; Figure 1). The rift-bounding fault system is best described as a series of 170–230 km long, N-S to NNW-SSE trending, east-dipping, eastward-stepping, first-order normal fault segments with throws up to ~5 km (e.g., Surlyk, 2003). These first-order segments are separated by a series of east-directed jogs, or steps, each of which shifts the rift-bounding fault system eastward by 25–100 km (e.g., Peacock et al., 2000). In East Greenland between 70 and 77°N, we define four first-order segments of the rift bounding fault system (segments 1–4), separated by three first-order eastward steps (steps A–C; Figure 1). The criteria for defining the four first-order segments have been to identify rift-bounding faults that are significant in the sense that they are well-documented in the literature and that they form the western structural boundary of Paleozoic to Mesozoic rift-related deposits. Furthermore, the rift-bounding fault segmentation proposed here is fully consistent with Surlyk's (2003, see their Figure 2) map of the Jurassic rift structure. Segment 1 is composed of the Stauning Alper Fault and its southern continuation (e.g., Haller, 1971) and stretches

~180 km N-S across Jameson Land from Scoresby Sund to Kong Oscar Fjord (Figure 1). The fault system comprised by segment 1 has appeared on maps at least since Haller (1971) and appears on maps in several more recent publications (Hartz et al., 2002; Henriksen, 1985; Henriksen, 2003; Surlyk, 2003). The Stauning Alper Fault has been active since the Paleozoic and was a significant structure by Permian times, when it formed the western structural boundary to a wide N-S trending embayment (Stemmerik et al., 1991). Segment 2 runs ~230 km N-S along Hold with Hope and Th. Thomsen Land (Figure 1) and is composed of the Post Devonian Main Fault (Vischer, 1943) and its northward continuation (see also Haller, 1971, where the northern part of segment 2 is described as a "Paleozoic fault system"; Surlyk et al., 1981; Larsen, 1988; Surlyk, 2003). It is separated from segment 1 by step A (Figure 1), which is a NE-trending fault that runs ~65 km across Traill Ø and Geographical Society Ø (e.g., Henriksen, 2003; Surlyk, 2003), and which had formed and was active by Devonian-Carboniferous times (Stemmerik et al., 1991). Segment 3 is the ~170 km long, NNW-ESE trending Clavering-Dombjerg Thomsen Land Fault system (Figure 1), which saw significant activity during the well-documented Late Jurassic to Early Cretaceous rift phase (Henstra et al., 2016; Kristensen et al., 2016; Surlyk & Korstgård, 2013); earlier activity (Carboniferous-Permian?) has also been suggested for this fault system (op. cit.). Segment 3 is separated from segment 2 by step B (Figure 1), which is a 25–40 km eastward shift of the rift boundary fault system across Clavering Ø (see Peacock et al., 2000). Segment 4 runs 50–100 km (offshore continuation uncertain) NNW-SSE along Store Koldewey (Haller, 1971; Larsen, 1988; Peacock et al., 2000; Surlyk, 2003; Surlyk et al., 1981) and is separated from segment 3 by a 50–60 km eastward step (step C; Figure 1).

This study is focused around samples from outcrops of the Dombjerg Fault, which forms part of the CDTF system (Kristensen et al., 2016; Surlyk & Korstgård, 2013), termed segment 3 in the rift fault framework outlined above (Figures 1, 3, and 4). The CDTF system comprises alternating NW/NNW-trending and NNE-trending segments, and the Dombjerg Fault is today connected with the Thomsen Land Fault by a NE-striking "transfer" fault, forming a pronounced dogleg in the map-view geometry of the fault system (Figures 1 and 3; Surlyk & Korstgård, 2013). The fault system forms the western bounding fault of a tilted half-graben syn-rift basin of

Upper Jurassic to Lower Cretaceous age (Wollaston Forland Basin; Henstra et al., 2016; Surlyk, 1978, 1984) and separates coarse-grained deep-water clastics in its hangingwall from Caledonian migmatite gneisses, amphibolites, and pegmatites in its footwall (Figures 3 and 4).

4. K-Ar Dating of Illite From Fault Gouges

The first application of K-Ar dating to clay minerals grown syn-kinematically in fault zones dates back more than 40 years (Lyons & Snellenburg, 1971). However, only in the last 15 years, thanks to advances in laboratory techniques and our understanding of fault zones, has the method emerged as a dating tool that is routinely used on shallow crustal faults (e.g., Löbens et al., 2011; Solum et al., 2005; Torgersen et al., 2014; van der Pluijm et al., 2001; Viola et al., 2016; Zwingmann et al., 2010). During fault movement, grain comminution (increase in surface area) and hydrothermal circulation, most likely also temperature and strain, all facilitate the growth of clay minerals, among them K-bearing and therefore datable illite (Vrolijk & van der Pluijm, 1999; Yan et al., 2001). These neocrystallized clays are typically mixed with finely crushed host rock material, which may also contain K-bearing mineral phases (illite, muscovite, K-feldspar, and hornblende). A potential contamination with host rock material must therefore be considered when interpreting illite fault gouge ages.

If fault gouges are developed in sedimentary host rocks, they generally contain both newly grown clays and detrital clays incorporated from the host rock, necessitating careful analyses to separate the two and obtain a reliable age for the faulting (Solum et al., 2005; van der Pluijm et al., 2001). In contrast, magmatic and high-grade metamorphic host rocks are inherently free of primary clay minerals; thus, all clays in fault gouges must have grown in the faults, making the interpretation of the obtained ages easier (Zwingmann et al., 2010; Zwingmann & Mancktelow, 2004). However, even faults in crystalline host rocks can show widely dispersed age spectra when several grain size fractions are dated, generally with ages decreasing with grain size. This age-grain size correlation is most commonly explained by contamination with K-bearing minerals from the wall rock, affecting the coarse grain size fractions to a larger degree, or by fault reactivation and mixing of several populations of illite (e.g., Ksienzyk et al., 2016; Torgersen et al., 2014; Viola et al., 2016; Zwingmann et al., 2010; Zwingmann & Mancktelow, 2004).

Five fault gouge samples were collected for K-Ar illite dating (Figures 4 and 5). All samples were taken from gouge zones along discrete strands of the Dombjerg Fault Zone in the crystalline basement of the footwall (Figure 4, annotated G1–G5). Due to their close spacing, we considered the faults to be cogenetic. The samples were dispersed in distilled water and separated into three grain size fractions of 2–6 μm , <2 μm , and <0.2 μm by gravitational settling in water and centrifugation. The mineralogy of the samples was determined by X-ray diffraction analyses on both air-dried and ethylene glycol solvated sample mounts, and the illite crystallinity was obtained by measuring the width at half the maximum height of the illite 10 Å peak (Kübler, 1964, 1967). For the K-Ar dating, K was measured in duplicate by flame photometry on one aliquot of each sample, while Ar was extracted from another aliquot by fusing the sample in a vacuum line, then analyzing the Ar isotopic composition by mass spectrometer. The details of the analytical procedure are identical to those described by Löbens et al. (2011).

4.1. K-Ar Sample Descriptions

In the study area, the Dombjerg Fault is relatively straight in map view and comprises a cross-sectional structure characterized by an ~600-m-wide damage zone in the Caledonian basement footwall and an ~500-m-wide damage zone affecting the Mesozoic clastics of the hangingwall (Kristensen et al., 2016). Slip appears to have been localized along discrete fault strands in the innermost 200 m of the footwall damage zone (we refer to this 200-m-wide zone as the central fault zone, following Childs et al., 2009); these fault strands are characterized by assemblages of fault rock that include a central zone of fault gouge ranging in width from ~5 to 50 cm, commonly enveloped by striated slip surfaces and fault breccias (Figure 5). For a full discussion of the fault zone architecture of the Dombjerg Fault, see Kristensen et al. (2016). Five fault gouge samples were collected from four different strands within the central fault zone of the Dombjerg Fault; the sample locations are shown in Figure 4. All of the sampled strands feature wall rocks of Caledonian crystalline “basement” rocks; none of the sampled strands feature wall rocks of Mesozoic sediments. Sample G1 was collected in the NW part of the study area from a fault strand characterized by wall rocks of dark, banded gneisses (Figure 5c). Near the fault strand, the wall rocks were intensely brecciated around an up to 50-cm-wide

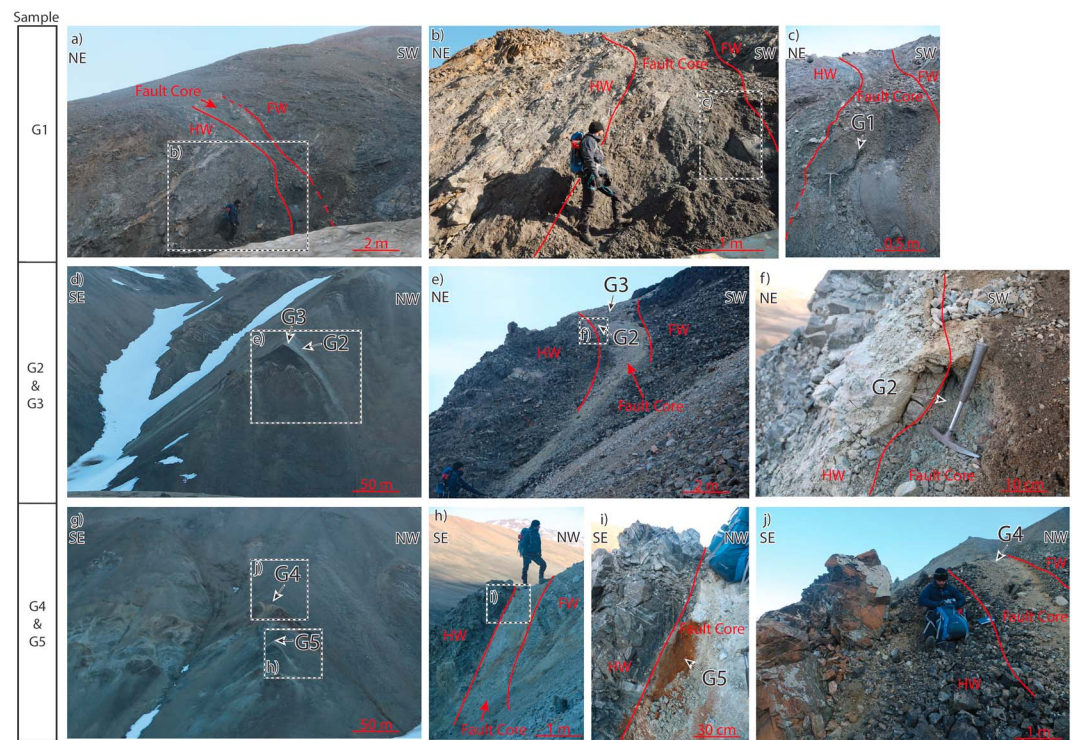


Figure 5. Outcrop photographs showing the sample locations of gouge samples collected for K-Ar illite dating. Sample locations are shown at progressively greater detail from left to right, and locations of close-ups are shown on the images: (a–c) Sample location G1; (d–f) sample locations G2 and G3; (g–j) sample locations G4 and G5.

zone of fault gouge. Several discrete slip surfaces were evident in and around the gouge zone. Samples G2 and G3 were collected from a rich gouge zone within a fault strand to the SE of G1 (Figures 5d and 5f); this fault strand was characterized by a hangingwall of felsic banded gneiss and a footwall of mafic to ultramafic rocks containing olivine, serpentine, and talc. Samples G4 and G5 were sampled from two separate but closely spaced (50 m) fault strands with abundant fault gouge further to the SE of samples G2 and G3 (Figures 5g and 5j). Wall rocks in this area were obliterated by fracturing and brecciation but consisted largely of banded gneisses.

4.2. K-Ar Results and Interpretation

X-ray diffraction analyses revealed that all samples contain illite, with chlorite and/or kaolinite as additional clay phases (Table 1). Only one sample (G1) shows traces of smectite. All samples contain variable amounts of quartz in the coarse fraction, and samples G2–G4 additionally have minor amounts/traces of plagioclase in their coarse fractions. Illite crystallinities (Kübler Index, KI; Kübler, 1964) mostly range from 0.4 to 0.8 $\Delta^{\circ}2\theta$, indicating illite crystallization between ~ 100 and 200°C (e.g., Merriman & Frey, 1999). Exceptions are the coarse and medium fraction of sample G1 and coarse fraction of sample G3, which have lower KI values between 0.26 and 0.4 $\Delta^{\circ}2\theta$, suggesting higher temperatures (200 – 300°C ; e.g., Merriman & Frey, 1999) during illite growth. Potassium contents range from 3.2 to 7.8 wt % K_2O and radiogenic ^{40}Ar from 33.5 to 91.1%, indicating reliable analytical conditions for all samples. K-Ar ages range from early Mississippian (350 Ma) to Late Triassic (236 Ma).

All samples show inclined age spectra with the age decreasing with grain size (Figure 6 and Table 1). This pattern is commonly explained either by mixing of an older age component inherited from the host rock with a younger generation of illite that crystallized in the fault or by mixing of older and younger illite generations that grew during different periods of fault initiation and reactivation (Torgersen et al., 2014; van der Pluijm et al., 2001; Viola et al., 2016; Zwingmann & Mancktelow, 2004). Since all faults are hosted in high-grade metamorphic crystalline host rocks, a contamination of the samples with detrital illite can be excluded; all illite in the samples must have grown in the faults. While illite can be difficult to distinguish from muscovite by X-ray diffraction analyses, petrographic thin sections showed only traces of muscovite in the host rocks.

Table 1
Mineralogy, Illite Crystallinity and K-Ar Data of Fault Gouge Samples

Sample	Fraction	Illite crystallinity ^a			Mineralogy ^b							K-Ar dating ^c				
		KI _a	KI _g	Zone	Ill	I/S	Chl	Kln	Qtz	Plg	FeS	K ₂ O (wt %)	⁴⁰ Ar* (nl/g) STP	⁴⁰ Ar* (%)	Age (Ma)	2σ (Ma)
G1	2–6 μm	0.32	0.26	Anchizone	+	?	+++	–	o	–	–	3.2	33.5	97.8	299	4
	<2 μm	0.39	0.37	Anchizone	+	o	+++	–	–	–	–	4.0	38.1	93.9	272	5
	<0.2 μm	0.61	0.58	Diagenetic zone	++	o	+++	–	–	–	–	4.5	36.6	92.6	236	3
G2	2–6 μm	0.52	0.45	Diagenetic zone	+++	–	+	++	+++	+	–	4.5	48.1	98.7	307	5
	<2 μm	0.72	0.71	Diagenetic zone	+++	–	+	++	–	–	–	6.6	68.5	92.8	295	5
	<0.2 μm	0.78	0.80	Diagenetic zone	+++	–	o	+	–	–	–	6.8	66.9	90.7	284	3
G3	2–6 μm	0.39	0.32	Anchizone	+++	–	+	++	+++	o	–	4.1	44.7	98.3	309	3
	<2 μm	0.64	0.61	Diagenetic zone	+++	?	o	++	–	–	–	6.3	63.3	95.5	287	3
	<0.2 μm	0.71	0.71	Diagenetic zone	+++	?	o	+	–	–	–	6.4	60.6	93.6	273	3
G4	2–6 μm	0.51	0.45	Diagenetic zone	+	–	o	+	+++	o	+	3.4	36.3	98.1	303	6
	<2 μm	0.68	0.64	Diagenetic zone	+++	–	o	++	–	–	–	6.4	64.0	93.8	288	7
	<0.2 μm	0.73	0.66	Diagenetic zone	+++	–	o	+	–	–	–	6.7	64.2	91.9	276	3
G5	2–6 μm	0.62	0.58	Diagenetic zone	+++	–	–	+	+	o	–	6.2	76.9	99.3	350	5
	<2 μm	0.65	n/a	Diagenetic zone	+++	–	–	+	–	–	–	7.8	91.1	97.7	331	7
	<0.2 μm	0.78	0.72	Diagenetic zone	+++	–	–	+	–	–	–	7.4	81.3	96.5	312	7

Note. Minerals: Ill, illite; I/S, interlayered illite-smectite; Chl, chlorite; Kln, kaolinite; Qtz, quartz; Plg, plagioclase; FeS, iron sulfides.

^aKübler Index (Δ^{20}) for air-dried (KI_a) and ethylene glycol-solvated (KI_g) sample mounts and equivalent metapelitic zone. ^b+++ , main component; ++, significant component; +, minor component; o, traces; ?, uncertain; –, not detected. ^cAr*, radiogenic argon; STP, standard temperature and pressure conditions.

Furthermore, the KI values of the fault gouge samples are much too high for muscovite from the high-grade metamorphic host rocks; we therefore rule out any significant contamination with muscovite from the host rock. None of the samples contained other K-bearing minerals (K-feldspar and hornblende). With the possibility of contamination by inherited material from the host rocks thus excluded, the K-Ar ages should correspond to slip episodes along the Dombjerg Fault.

When interpreting inclined age spectra in terms of fault reactivation, the coarsest fraction with the oldest ages is generally interpreted as the age of fault initiation (Torgersen et al., 2014; Viola et al., 2016). Strictly, this is a minimum age, since some mixing with younger illite grown during fault reactivation might occur. The finest fraction with the youngest age is correspondingly interpreted as the age of the latest illite growth during fault reactivation. This should generally be considered a maximum age for fault reactivation, since some mixing with older illite from earlier fault activity is possible. Ages from intermediate grain size fractions are mostly mixed ages between these two end members and have little geological relevance.

The oldest, Early Mississippian, age comes from the coarse fraction of sample G5 (Figure 6 and Table 1). We interpret this age as the minimum age for brittle fault initiation in Late Devonian or Early Mississippian times (>350 Ma). The fine fraction of G5 yielded a Middle Pennsylvanian age (312 Ma), which overlaps, within the uncertainties, with the coarse fraction ages of samples G2, G3, G4, and G5 (309–299 Ma). The latest Carboniferous must thus have been a period of considerable fault activity, causing reactivation of the fault strand represented by sample G5. The other four sampled faults either first developed into brittle gouge-bearing faults at this time or, if they were already active contemporaneously with G5 in the early Carboniferous, late Carboniferous activity was so extensive that all previous isotopic signals were erased. A second Paleozoic period of significant fault activity in the Middle Permian (284–273 Ma) is documented by the fine fraction ages of samples G2, G3, and G4 (Figure 6 and Table 1). Only one fault (sample G1) recorded any indication of Mesozoic fault movement. We interpret the Late Triassic age of the fine fraction as a maximum age for Late Triassic or younger (<240 Ma) fault reactivation.

The potential for excess argon in the samples, which is a known challenge in K-Ar and Ar-Ar dating techniques (see e.g., Kelley, 2002), is considered to be very minor. While it is *theoretically* possible that the samples may have been affected by excess argon, it is highly unlikely that several samples give the same age unless that age represents a real geological event. This would require exactly the same amount of contamination with excess argon in all samples. In case of the late Carboniferous age, all five samples have ages that overlap within their uncertainties, and three samples support the Middle Permian event; this gives confidence in the

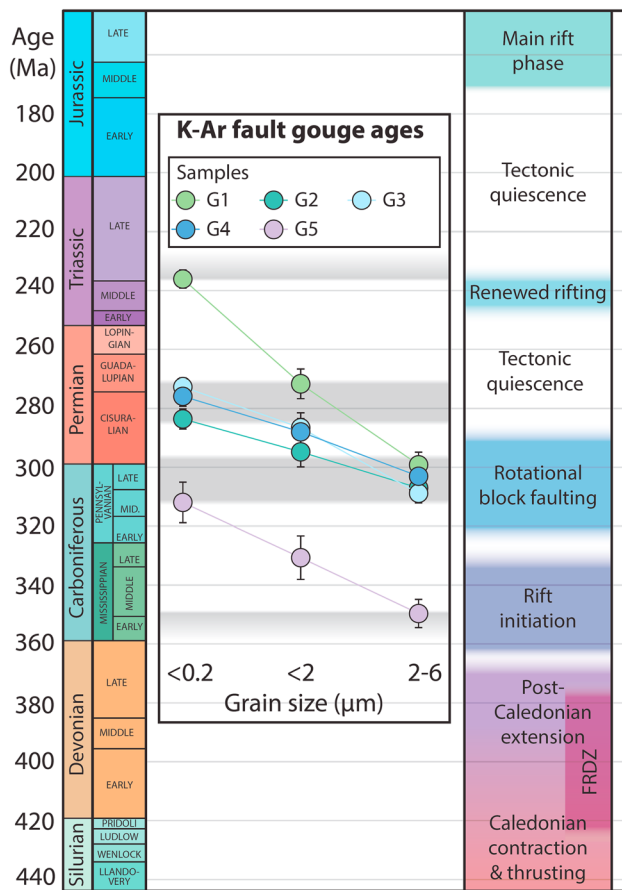


Figure 6. Results from K-Ar age dating of illite from fault gouge samples (refer to Figure 4 for location) shown for different grain size fractions. Uncertainties are $\pm 2\sigma$. Coarse fraction (2–6 μm) ages date fault initiation or an older fault event; fine fraction (<0.2 μm) ages date fault reactivation. Note that the intermediate grain size fraction (<2 μm) generally yields mixed ages of little geological significance. Samples G1–G5 display mainly Pennsylvanian to Middle Permian ages, but with some indication of earlier (Mississippian or older) and younger (Late Triassic or younger) illite growth. Four periods of fault activity are identified based on the K-Ar ages and are represented by gray bars (see text for full discussion). The right column shows key tectonic events in East Greenland rift system (see text for references). FRDZ = Fjord Region Detachment Zone.

results. The Early Mississippian (or older) brittle fault initiation and Late Triassic (or younger) fault reactivation are represented by only one age each and are consequently interpreted as minimum and maximum ages for these events, respectively.

5. Discussion and Conclusions

5.1. Geological Significance of the Recorded K-Ar Ages

The K-Ar illite ages recorded in the five samples shed light on the history of the studied fault system prior to the well-documented main Jurassic-Cretaceous rift event (Henstra et al., 2016; Surlyk, 1978, 1984, 1990, 2003; Surlyk & Korstgård, 2013), defining four periods of fault activity in the Late Paleozoic to Early Mesozoic: (i) a minimum age of brittle fault initiation in the early Mississippian (>350 Ma), (ii) significant activity affecting all dated faults and causing abundant illite crystallization in the Middle-Late Pennsylvanian (ca. 310–300 Ma), (iii) a second period of significant fault reactivation in the Middle Permian (ca. 280–270 Ma), and (iv) some indication of Middle Triassic or younger (<240 Ma) fault reactivation (Figure 6).

The well-documented Jurassic-Cretaceous rift event itself, with up to 3 km of throw, recorded by sedimentary growth packages in the hangingwall (e.g., Henstra et al., 2016; Surlyk & Korstgård, 2013), is not recorded in the K-Ar illite data. This was to be expected, however, since conditions were not likely favorable for the crystallization of illite during this rift phase: At this time, the Dombjerg Fault Zone was a surface-breaching growth fault as it was accumulating sediments in the hangingwall (e.g., Henstra et al., 2016). The exposed structural level was therefore at or near the surface at the time of faulting; consequently, wall rock temperatures must have been low. In sedimentary rocks, illite (as mixed layer illite-smectite) starts to grow at temperatures of 40–70°C; discrete illite, as found in our samples, occurs above ~100°C, that is, at several kilometers depth (Hower et al., 1963; Jennings & Thompson, 1986; Srodon & Eberl, 1984). Failure of the K-Ar or Ar-Ar illite system to record the youngest fault activity has been attributed to insufficient temperatures for illite growth before (Duvall et al., 2011; Pleuger et al., 2012), but never has a case been so clearly documented as in the Dombjerg Fault Zone, where Jurassic-Cretaceous movement is perfectly recorded in the sedimentary record (e.g., Henstra et al., 2016; Surlyk, 1978), yet could not be detected in the analyzed fault gouge samples at all. An alternative, but in our view less likely, explanation

for the lack of Jurassic-Cretaceous K-Ar ages would be that fault activity shifted to nonsampled fault strands, for example, in the nonexposed contact zone between basement and syn-rift sediments, and that the sampled fault strands were not reactivated in the Middle Jurassic-Early Cretaceous event.

5.2. Timing of Paleozoic Activity on the Clavering-Dombjerg-Thomsen Land Fault System in Context of the East Greenland Rift System as a Whole

Based on K-Ar illite ages, activity on the CDTF system (segment 3; see Figure 1) most likely initiated in Mississippian times, concurrent with what most authors suggest as the onset of E-W directed extension that led to the protracted development of the East Greenland Rift in Paleozoic to Mesozoic times (e.g., Larsen, 1988; Stemmerik et al., 1991; Surlyk, 1990, 2003). Along segment 2 of the rift boundary fault network (Figure 1), Mississippian Ar-Ar mineral cooling ages, reported in Hartz et al. (2006), indicate accelerated cooling/exhumation and are consistent with extensional fault activity at the time. Further support for fault-driven denudation following Mississippian onset of rift fault activity is found in apatite fission track data from SW Clavering Ø (Johnson & Gallagher, 2000), indicating crustal cooling and exhumation since the

Carboniferous. Further south, Stemmerik et al. (1991) argue, based on biostratigraphic data, that the step A segment at Traill Ø and Geographical Society Ø (Figure 1) was also active in the Mississippian and possibly earlier (Devonian). Assuming that step A represents a mega-linkage of segments 1 and 2 (cf. Peacock et al., 2000), the evidence from Stemmerik et al. (1991) and the K-Ar data from this study combined indicate that, already in Mississippian times, the western rift-bounding fault system of the East Greenland Rift was a structure evolved to an advanced level and that strain at this time had probably localized onto a few large, regionally significant fault systems (cf. Cowie et al., 2005; Gawthorpe et al., 2003). Furthermore, it shows that the rift itself had developed as a regionally significant structure along much of its present strike length already by Mississippian times. This is an interesting finding, since most previous studies suggest a Pennsylvanian to Early Permian age for the main Paleozoic rift phase, during which rotational block faulting took place (Figure 6; Haller, 1971; Larsen, 1988; Surlyk et al., 1984, 1986). The main Middle-Late Pennsylvanian phase of movement of the CDTF identified from the K-Ar data agrees well with this Late Carboniferous to Early Permian rift phase, and its strong signature in the data suggests that it is indeed the most significant Paleozoic rift phase, although not the earliest one. A Middle Permian period of fault activity, as suggested by the K-Ar fault gouge data, may represent the waning stages of the Carboniferous to Early Permian main rift phase and may extend the duration of this rift phase further into the Permian than suggested previously. However, it may also represent a separate reactivation event not previously recorded or described in East Greenland. Middle Permian fault activity is known from other parts of the North Atlantic margin system, for example, in Western Norway (Ksienzyk et al., 2016; Viola et al., 2016).

The younger Middle Triassic illite age, although only recorded in the smallest grain size fraction of one sample (Figure 6), could reflect reactivation during the postrift stages of Early Triassic rifting, which was a significant event across the North Atlantic (Clemmensen, 1980; Müller et al., 2005; Steel & Ryseth, 1990). On the Middle Norwegian shelf, a shift occurs in the postrift stage in late Ladinian times, from inactivity to slip on key faults (Müller et al., 2005). A similar onset of fault activity in Middle-Late Triassic has not been documented in East Greenland before. While the single Middle Triassic K-Ar age from this study might indicate that parts of the East Greenland Rift have experienced renewed fault activity at the time, further sampling would be needed to test this hypothesis.

5.3. The Role of Structural Inheritance in the East Greenland Rift System

It is well known from other rift systems that preexisting structural fabric plays an important role during rifting and may place strong control on the nucleation, localization, growth, reactivation, segmentation, and overall structure of rift basins and related fault systems (e.g., Duffy et al., 2015; Ebinger et al., 1997; Gibson et al., 2013; Henstra et al., 2015; Milani & Davison, 1988; Miller et al., 2002; Moustafa, 1997; Salomon et al., 2015; Theunissen et al., 1996; Whipp et al., 2014). This has only to a very limited extent been previously discussed for the East Greenland Rift. As we will argue in the following, however, there are several lines of observation and evidence that suggest that structural inheritance has played an important role for the structure and evolution of the Paleozoic to Mesozoic rift system of East Greenland.

In the area of the CDTF, there is spatial and temporal coincidence between older syn- to late Caledonian extensional faults/shear zones and the younger rift structures. The KSZ (Dallmeyer et al., 1994; Gilotti & McClelland, 2008), located in the Ardencaple Fjord area to the NW of Wollaston Forland (Figure 1), is a crustal scale mylonitic shear zone along which middle to lower crustal rocks were unroofed during the late stages and after Caledonian contraction. The KSZ is proposed to continue SE-ward from Ardencaple Fjord toward Wollaston Forland (Henriksen, 2003), where its NNW trend coincides with the trend of the Dombjerg Fault (Figures 1, 3, and 4). There are several observations that suggest interaction between the older KSZ and the younger Paleo-Mesozoic rift fault system, represented here locally by the CDTF.

First, the strike orientation of the NNW- to NW-trending Dombjerg Fault deviates from the overall rift trend (N-S) but is parallel to the strike of the SE-ward continuation of the KSZ (Figures 1 and 4). This may suggest that the CDTF locally inherited and adopted the KSZ strike orientation. At depth, however, we argue that the CDTF must truncate and offset the KSZ, given the contrasting dips between the low-angle extensional detachment of the KSZ and the steep CDTF, and the presence of both structures at the surface (Figure 7). This is similar to what was proposed for the relationship between some intrabasement structures and younger rift fabric offshore southern Norway, termed “cross-cutting fault interaction” by Phillips et al. (2016; Figure 8). Despite the fact that intrabasement structures are cross-cut and offset by the steeper-dipping

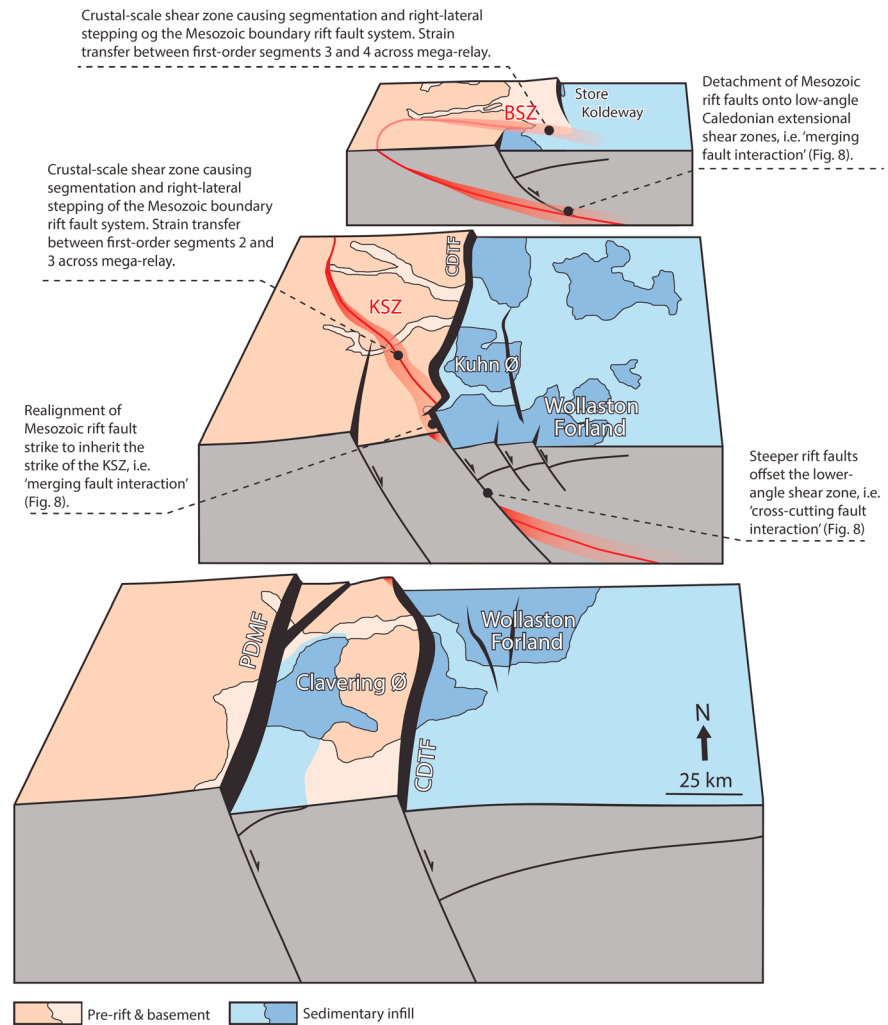


Figure 7. Schematic three-dimensional block diagrams showing the proposed relationship between the preexisting Caledonian extensional shear-zones and the younger rift fault network. See Figure 1 for approximate location. The top block diagram shows Bessel Fjord area, highlighting the co-location of the Bessel Fjord shear zone and the right-lateral step C between rift fault segments 3 and 4 (see also Figure 1 for an overview of the rift fault network). The Bessel Fjord shear zone represents a crustal-scale heterogeneity that induces segmentation of the rift system. Note also the relationship at depth where the steep normal fault (segment 3 of the rift fault network shown in Figure 1) hypothetically detaches onto the Bessel Fjord shear zone. See text for full discussion. The middle block diagram shows the Ardencaple Fjord-Wollaston Forland area, where the Kildedalen Shear Zone (KSZ) similarly causes the right-lateral step B between rift fault segments 2 and 3. Furthermore, note that the rift faults locally adopt the strike orientation of the KSZ. Note also, given the low-angle nature of the KSZ and the steep nature of the rift faults, that the KSZ is truncated and offset by the rift faults into its hangingwall. The lowermost block diagram shows the southward continuation of the fault system for completeness. See text for full discussion.

younger faults, this form of interaction clearly involves structural inheritance (of fault strike, in this case). We hypothesize, however, that the style of interaction between the low-angle Caledonian shear zones and the rift fault network may vary spatially and that rift fault segments may also locally root and detach onto the extensional detachments (Figure 7). This is similar to what was termed “merging fault interaction” by Phillips et al. (2016; Figure 8) and supports their notion that the style of interaction between “basement” fabric and younger rift structure may vary greatly within rifts.

Second, the locations of the eastward steps (steps B and C; Figure 1) of the rift fault system coincide with the location of the SE-ward continuations of the KSZ and the BSZ, respectively (Figures 1 and 7). Controls of “basement” fabric on rift segmentation and the location of regional transfer zones are widely accepted (e.g., Acocella et al., 1999; Fossen & Rotevatn, 2016; Morley et al., 1990) and have previously been

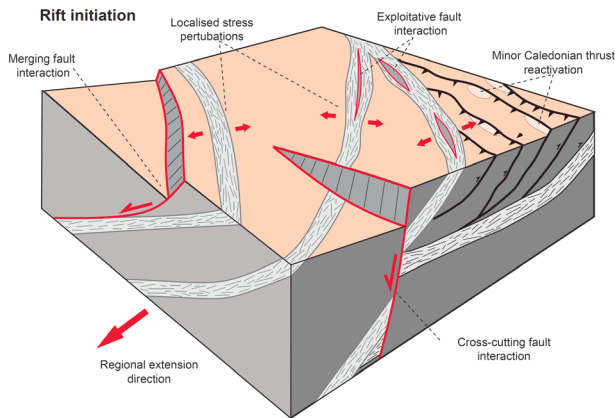


Figure 8. Synoptic figure modified from Phillips et al. (2016) showing how the presence of discrete intrabasement structures may modify the geometry and evolution of overlying rift systems. During extension, preexisting intrabasement structures (shown as thick zones with planar parallel fabric) act to create localized perturbations in the regional stress field, producing a range of interactions with the rift-related faults (shown as gray surfaces with red traces).

documented or proposed in several rift basins, including the Suez Rift (Khalil & McClay, 2001; Moustafa, 1997; Younes & McClay, 2002) and the North Sea Rift (Faereth & Ravnås, 1998; Fossen et al., 2017).

Third, the KSZ was active until at least 380 Ma, possibly even to 370 Ma, based on Ar-Ar muscovite and hornblende cooling ages from Dallmeyer et al. (1994); thus, only 20–30 Ma separate the activity on the KSZ from the oldest K-Ar ages from the Dombjerg Fault recorded in this study. This may suggest that the KSZ represented a crustal fabric that was relatively young, and therefore weak and more susceptible to reactivation during rifting (cf. Tenthorey et al., 2003).

Similar relationships can be seen further south in the East Greenland rift system. In the Forsblad Fjord Area (Figure 1), the regionally significant FRDZ (Andresen et al., 1998) is represented locally by the Højedal and Tindern Detachments (White et al., 2002; Figure 1). White and Hodges (2003) show that the Højedal Detachment was active 414–380 Ma (i.e., Siluro-Devonian), then again at 357 Ma (i.e., earliest Carboniferous), based on Ar-Ar thermochronology. The Højedal Detachment sits in a similar structural position to that of KSZ and shows a similar coincidence with rift structure and segmentation as presented

above for the Wollaston Forland area: First, the location of the Forsblad Fjord area and the Højedal Detachment broadly coincides with the location of another major eastward step (step A) of the rift, from segment 1 (Scoresby Sund-Kong Oscar Fjord) to segment 2 (Hold With Hope) along the NE-trending transfer fault cross Traill Ø and Geographical Society Ø (Figure 1). Second, the latest activity along the Højedal Detachment (357 Ma; White & Hodges, 2003) coincides and overlaps with the age of the earliest rift-related deposits in the hangingwall of the NE-trending transfer fault at Traill Ø and Geographical Society Ø, which has been biostratigraphically dated to the latest Devonian to early Carboniferous (Stemmerik et al., 1991).

In summary, the close temporal and spatial relationships between low-angle Caledonian shear zones and the younger rift fabric provide compelling evidence that the Caledonian structural grain strongly influenced rift development in Paleozoic to Mesozoic times. Specifically, we suggest that “basement” heterogeneity related to the Caledonian structural grain placed strong controls on (i) the localization, nucleation, and orientation of rift faults and (ii) the location of regionally significant transfer zones and therefore also (iii) constrained the length and location of first-order segments of the Paleozoic-Mesozoic rift fault system. The close coincidence in time between (i) the latest activity (357 Ma; White & Hodges, 2003) on the preexisting network of extensional low-angle mylonitic shear zones responsible for the syn- to postorogenic exhumation of the Caledonian crust on the one hand, and (ii) the earliest activity on the rift fault network (latest Devonian to earliest Carboniferous; e.g., Stemmerik et al., 1991; Surlyk, 1990, 2003) on the other, leads us to hypothesize that the preexisting network represented a fresh and weak structural grain (cf. Tenthorey et al., 2003) that acted as a template for the establishment of the East Greenland rift system. The fact that the East Greenland rift system was active along much of its present-day N-S extent already in Mississippian times suggests that it attained its final length quickly, which is another strong argument for structural inheritance of an underlying basement grain during fault growth (Jackson & Rotevatn, 2013; Nicol et al., 2017; Tvedt et al., 2016; Walsh et al., 2003). In addition to the influence of the known Caledonian extensional shear zones discussed in this paper, which imparts a strong control on rift segmentation and transfer zones, we therefore speculate that the N-S trending East Greenland rift system may follow other (N-S trending) Caledonian basement structures that are hidden at depth. One likely suspect would be thrusts (or thrusts reactivated as extensional detachments) at depth (cf. Phillips et al., 2016); the Caledonian thrust front located 200–400 km west of the rift-bounding fault system strikes N-S to NNE-SSW (e.g., Henriksen, 2003), consistent with the strike of the East Greenland rift system, and similar striking (reactivated) thrusts may have influenced the overall localization and strike of the rift.

5.4. Concluding Remarks and Implications for the Time Scales of Rift Propagation, Border Fault Growth, and Rift Length Establishment

The findings of the present study demonstrate that structural inheritance are of great significance in determining the structure not only of faults (e.g., Autin et al., 2013; Corti et al., 2007; Fossen et al., 2017; Henstra

et al., 2015; Michon & Sokoutis, 2005; Phillips et al., 2016; Worthington & Walsh, 2011) but also of entire rift systems as they evolve, including (i) the localization of faults and (sub)basins, (ii) the localization and spacing of rift-scale transfer zones, and thereby (iii) the length and segmentation of master faults that control overall basin geometry and physiography in rifts. Ultimately, overall rift geometry and segmentation may largely be determined by inheritance of preexisting structural fabric, which underpins the importance to constrain the configuration of such fabric in order to understand its relationship with overlying rift structure.

The closeness in time between the latest activity on the Caledonian basement structures and the younger rift structure seen in this study may suggest that structural inheritance may be particularly important in presence of a relatively young, and therefore weak, crustal fabric during rifting. With time, faults and shear zones may recover their strength (e.g., Tenthorey et al., 2003), which means that a younger crustal fabric may be weaker and more susceptible to interaction with subsequent rift events.

The fact that the East Greenland rift system attained its length early in its life bears similarity to the behavior seen in many normal fault systems at a smaller (fault array to individual fault) scale, whereby faults also attain their near full length at an early stage before subsequently accruing displacement. This mode of normal fault growth is termed the “coherent fault model” (Jackson & Rotevatn, 2013; Walsh et al., 2003) or, more recently, the “constant-length model” (Jackson et al., 2017; Nicol et al., 2005, 2017; Rotevatn et al., 2018). Rotevatn et al. (2018) suggest that most normal faults spend 20–30% of their slip history attaining their near full length, before accruing displacement for the remaining 70–80% of their lifetime. Assuming the southcentral part of the East Greenland rift system initiated in the latest Devonian (ca. 370–360 Ma; Stemmerik et al., 1991) and was established along most of its length by Mississippian times (ca. 350 Ma as recorded by sample G5 in this study; see Table 1), the rift grew to its near-full length within the first 10–20 Myr of its lifespan. If we consider the end of the main Paleozoic rift phase in Early Permian times (ca. 270 Ma), the rift lifespan amounts to ca. 100 Myr, and the rift system thus appears to have grown to its near-full length within 10–20% of its active history. If the end of the Middle Jurassic to Early Cretaceous rift phase (ca. 140 Ma) is considered as the end of rift life (extending the rift lifespan to ca. 230 Myr), the 10–20 Myr lengthening phase of the rift system amounts to 4–9% of its active history. Regardless of what is considered the end of rift life, rapid lengthening (10–20 Myr; 4–20% of rift life) of the East Greenland rift system appears consistent with the predictions of the “constant-length model” for normal fault growth (see e.g., Jackson et al., 2017; Nicol et al., 2017; Rotevatn et al., 2018). Rapid lengthening and establishment of rifts and their border fault systems is also seen in other rift systems globally. In the young (4–5 Ma) and presently active Corinth Rift, the growth of key fault systems has been constrained at 100-Kyr time scales, revealing rapid growth and establishment of a linked rift border fault system already <4–5 Myr into rift history (Nixon et al., 2016). Another example is the Baikal Rift proper, which has broadly occupied the same areal extent since shortly after its initiation in the Oligocene, possibly earlier (Mats & Perepelova, 2011). Our findings from the East Greenland rift system along with the support from these other examples indicate that rapid establishment of border fault systems and rift length is likely common, and not a feature restricted to the example studied herein. This leads us to tentatively suggest that the “constant-length model” for normal fault growth may be applicable also at the scale of entire rift systems. However, Nixon et al. (2016) also show that the establishment of border fault systems, albeit rapid, is characterized by tip propagation, relay breaching, and fault linkage, which is at variance with the “constant-length model” for fault growth (e.g., Nicol et al., 2005, 2017). This implies that hybrid growth behaviors, such as recently suggested for normal faults (Finch & Gawthorpe, 2017; Rotevatn et al., 2018) likely also apply at rift scale, whereby (i) a rapid stage of fault (or, in this case, rift) length establishment achieved through tip propagation, relay breaching, and fault linkage (i.e., “isolated fault growth”; see Jackson et al., 2017; Rotevatn et al., 2018) is followed by (ii) a stage of displacement accumulation and subsidence without significant further tip (or rift) propagation (i.e., “constant-length fault growth”; see Jackson et al., 2017; Rotevatn et al., 2018).

Acknowledgments

The authors wish to thank the WOLLGAN project consortium, and in particular J.P. Nystuen and E.P. Johannesen, for excellent collaboration on related sedimentological and basinal studies on Wollaston Forland. We are grateful to Norske Shell, who funded this study as well as the PhD projects of T.B. Kristensen and G.A. Henstra. We are particularly indebted to R. Ravnås (formerly Norske Shell) for his support. The LoCrA consortium is acknowledged for funding the participation of I. Midtkandal and S.A. Grundvåg in the field campaign. S.A. Grundvåg also received funding from the ARCEX project (Research Centre for Arctic Petroleum Exploration) which is funded by the Research Council of Norway (grant 228107). We thank the University of Otago (New Zealand), who hosted the lead author on a research sabbatical during which this paper was written. We also thank reviewers O. Duffy, E. Hartz, and T. Phillips, whose insightful comments helped improve this paper. We also appreciated the editorial guidance of C. Faccenna and J. Geissman. The new data presented in this paper are made available in Table 1. The University of Bergen and ARCEX are thanked for funding the open access publication of this paper.

References

- Acocella, V., Faccenna, C., Funicello, R., & Rossetti, F. (1999). Sand-box modelling of basement-controlled transfer zones in extensional domains. *Terra Nova-Oxford*, 11(4), 149–156. <https://doi.org/10.1046/j.1365-3121.1999.00238.x>
- Andresen, A., Hartz, E. H., & Vold, J. (1998). A late orogenic extensional origin for the infracrustal gneiss domes of the East Greenland Caledonides (72–74°N). *Tectonophysics*, 285(3–4), 353–369. [https://doi.org/10.1016/S0040-1951\(97\)00278-3](https://doi.org/10.1016/S0040-1951(97)00278-3)
- Andresen, A., Rehnström, E., & Holte, M. (2007). Evidence for simultaneous contraction and extension at different crustal levels during the Caledonian orogeny in NE Greenland. *Journal of the Geological Society*, 164(4), 869–880. <https://doi.org/10.1144/0016-76492005-056>

- Augland, L. E., Andresen, A., & Corfu, F. (2010). Age, structural setting, and exhumation of the Liverpool Land eclogite terrane, East Greenland Caledonides. *Lithosphere*, 2(4), 267–286. <https://doi.org/10.1130/L75.1>
- Autin, J., Bellahsen, N., Leroy, S., Husson, L., Beslier, M.-O., & d'Acremont, E. (2013). The role of structural inheritance in oblique rifting: Insights from analogue models and application to the Gulf of Aden. *Tectonophysics*, 607, 51–64. <https://doi.org/10.1016/j.tecto.2013.05.041>
- Bonini, M., Souriot, T., Boccaletti, M., & Brun, J. P. (1997). Successive orthogonal and oblique extension episodes in a rift zone: Laboratory experiments with application to the Ethiopian Rift. *Tectonics*, 16(2), 347–362. <https://doi.org/10.1029/96TC03935>
- Brune, S., Corti, G., & Ranalli, G. (2017). Controls of inherited lithospheric heterogeneity on rift linkage: Numerical and analog models of interaction between the Kenyan and Ethiopian rifts across the Turkana depression. *Tectonics*, 36, 1767–1786. <https://doi.org/10.1002/2017TC004739>
- Childs, C., Manzocchi, T., Walsh, J. J., Bonson, C. G., Nicol, A., & Schöpfer, M. P. J. (2009). A geometric model of fault zone and fault rock thickness variations. *Journal of Structural Geology*, 31(2), 117–127. <https://doi.org/10.1016/j.jsg.2008.08.009>
- Christiansson, P., Faleide, J. I., & Berge, A. M. (2000). Crustal structure in the northern North Sea: An integrated geophysical study. *Geological Society of London, Special Publications*, 167(1), 15–40. <https://doi.org/10.1144/GSL.SP.2000.167.01.02>
- Clemmens, L. B. (1980). Triassic rift sedimentation and palaeogeography of Central East Greenland. *Bulletin Grønlands Geologiske Undersøgelse*, 136, 1–72.
- Cocks, L., & Torsvik, T. (2002). Earth geography from 500 to 400 million years ago: A faunal and palaeomagnetic review. *Journal of the Geological Society*, 159(6), 631–644. <https://doi.org/10.1144/0016-764901-118>
- Corti, G., van Wijk, J., Cloetingh, S., & Morley, C. K. (2007). Tectonic inheritance and continental rift architecture: Numerical and analogue models of the East African Rift system. *Tectonics*, 26, TC6006. <https://doi.org/10.1029/2006TC002086>
- Coward, M. P. (1990). The Precambrian, Caledonian and Variscan framework to NW Europe. *Geological Society of London, Special Publications*, 55(1), 1–34. <https://doi.org/10.1144/GSL.SP.1990.055.01.01>
- Cowie, P. A., Underhill, J. R., Behn, M. D., Lin, J., & Gill, C. E. (2005). Spatio-temporal evolution of strain accumulation derived from multi-scale observations of Late Jurassic rifting in the northern North Sea: A critical test of models for lithospheric extension. *Earth and Planetary Science Letters*, 234(3–4), 401–419. <https://doi.org/10.1016/j.epsl.2005.01.039>
- Dallmeyer, R. D., Strachan, R. A., & Henriksen, N. (1994). 40Ar/39Ar mineral age record in NE Greenland: Implications for tectonic evolution of the North Atlantic Caledonides. *Journal of the Geological Society*, 151(4), 615–628. <https://doi.org/10.1144/gsjgs.151.4.0615>
- Duffy, O. B., Bell, R. E., Jackson, C. A. L., Gawthorpe, R. L., & Whipp, P. S. (2015). Fault growth and interactions in a multiphase rift fault network: Horda Platform, Norwegian North Sea. *Journal of Structural Geology*, 80, 99–119. <https://doi.org/10.1016/j.jsg.2015.08.015>
- Duvall, A. R., Clark, M. K., van der Pluijm, B. A., & Li, C. (2011). Direct dating of Eocene reverse faulting in northeastern Tibet using Ar-dating of fault clays and low-temperature thermochronometry. *Earth and Planetary Science Letters*, 304(3–4), 520–526. <https://doi.org/10.1016/j.epsl.2011.02.028>
- Ebinger, C., Djomani, Y. P., Mbede, E., Foster, A., & Dawson, J. B. (1997). Rifting Archaean lithosphere: The Eyasi-Manyara-Natron rifts, East Africa. *Journal of the Geological Society*, 154(6), 947–960. <https://doi.org/10.1144/gsjgs.154.6.0947>
- Færseth, R. B., Gabrielsen, R. H., & Hurich, C. A. (1995). Influence of basement in structuring of the North Sea basin, offshore southwest Norway. *Norsk Geologisk Tidsskrift*, 75, 105–119.
- Færseth, R. B., & Ravnås, R. (1998). Evolution of the Oseberg fault-block in context of the northern north sea structural framework. *Marine and Petroleum Geology*, 15(5), 467–490. [https://doi.org/10.1016/S0264-8172\(97\)00046-9](https://doi.org/10.1016/S0264-8172(97)00046-9)
- Finch, E., & Gawthorpe, R. (2017). Growth and interaction of normal faults and fault network evolution in rifts: Insights from three-dimensional discrete element modelling. *Geological Society of London, Special Publications*, 439(1), 219–248. <https://doi.org/10.1144/SP439.23>
- Fossen, H. (2010). Extensional tectonics in the North Atlantic Caledonides: A regional view. *Geological Society of London, Special Publications*, 335(1), 767–793. <https://doi.org/10.1144/SP335.31>
- Fossen, H., Khani, H. F., Faleide, J. I., Ksienzyk, A. K., & Dunlap, W. J. (2017). Post-Caledonian extension in the West Norway-northern North Sea region: The role of structural inheritance. *Geological Society of London, Special Publications*, 439(1), 465–486. <https://doi.org/10.1144/SP439.6>
- Fossen, H., & Rotevatn, A. (2016). Fault linkage and relay structures in extensional settings—A review. *Earth-Science Reviews*, 154, 14–28. <https://doi.org/10.1016/j.earscirev.2015.11.014>
- Friderichsen, J. (1999). Hard rock geology of Th. Thomsen Land, East Greenland Caledonides. *Danmark og Grønlands Geologiske Undersøgelse Rapport*, 1999(19), 111–119.
- Friderichsen, J. D., Henriksen, N., & Strachan, R. A. (1994). Basementcover relationships and regional structure in the Grandjean Fjord-Bessel Fjord region (75–76 N), North-East Greenland. *Rapport Grønlands Geologiske Undersøgelse*, 162, 17–33.
- Gawthorpe, R. L., Jackson, C. A. L., Young, M. J., Sharp, I. R., Moustafa, A. R., & Leppard, C. W. (2003). Normal fault growth, displacement localisation and the evolution of normal fault populations: The Hammam Faraun fault block, Suez rift, Egypt. *Journal of Structural Geology*, 25(6), 883–895. [https://doi.org/10.1016/S0191-8141\(02\)00088-3](https://doi.org/10.1016/S0191-8141(02)00088-3)
- Gee, D. G., Fossen, H., Henriksen, N., & Higgins, A. K. (2008). From the Early Paleozoic platforms of Baltica and Laurentia to the Caledonide Orogen of Scandinavia and Greenland. *Episodes*, 31(1), 44–51.
- Gee, D. G., & Sturt, B. (1985). *The Caledonide Orogen: Scandinavia and related areas*. Chichester, UK: Wiley.
- Giba, M., Walsh, J., & Nicol, A. (2012). Segmentation and growth of an obliquely reactivated normal fault. *Journal of Structural Geology*, 39, 253–267. <https://doi.org/10.1016/j.jsg.2012.01.004>
- Gibson, G. M., Totterdell, J. M., White, L. T., Mitchell, C. H., Stacey, A. R., Morse, M. P., & Whitaker, A. (2013). Pre-existing basement structure and its influence on continental rifting and fracture zone development along Australia's southern rifted margin. *Journal of the Geological Society*, 170(2), 365–377. <https://doi.org/10.1144/jgs2012-040>
- Gilotti, J. A., & McClelland, W. C. (2008). Geometry, kinematics, and timing of extensional faulting in the Greenland Caledonides—A synthesis. *Geological Society of America Memoirs*, 202, 251–271.
- Gudlaugsson, S. T., Faleide, J. I., Johansen, S. E., & Breivik, A. J. (1998). Late Palaeozoic structural development of the south-western Barents Sea. *Marine and Petroleum Geology*, 15(1), 73–102. [https://doi.org/10.1016/S0264-8172\(97\)00048-2](https://doi.org/10.1016/S0264-8172(97)00048-2)
- Haller, J. (1971). *Geology of the East Greenland Caledonides*. London: Interscience Publishers.
- Hartz, E., & Andresen, A. (1995). Caledonian sole thrust of central East Greenland: A crustal-scale Devonian extensional detachment? *Geology*, 23(7), 637–640. [https://doi.org/10.1130/0091-7613\(1995\)023%3C0637:CSTOCE%3E2.3.CO;2](https://doi.org/10.1130/0091-7613(1995)023%3C0637:CSTOCE%3E2.3.CO;2)
- Hartz, E., Kristiansen, S., Calvert, A., Hodges, K., & Heeremans, M. (2006). Structural, thermal and rheological control of the Late Paleozoic basins in East Greenland. *Proceedings of the Fourth International Conference on Arctic Margins* (pp. 58–76).
- Hartz, E. H., Andresen, A., Hodges, K. V., & Martin, M. W. (2001). Syncontractional extension and exhumation of deep crustal rocks in the East Greenland Caledonides. *Tectonics*, 20(1), 58–77. <https://doi.org/10.1029/2000TC900020>

- Hartz, E. H., Andresen, A., Martin, M. W., & Hodges, K. V. (2000). U-Pb and 40Ar/39Ar constraints on the Fjord Region Detachment Zone: A long-lived extensional fault in the central East Greenland Caledonides. *Journal of the Geological Society*, 157(4), 795–809. <https://doi.org/10.1144/jgs.157.4.795>
- Hartz, E. H., Eide, E. A., Andresen, A., Midboe, P., Hodges, K. V., & Kristiansen, S. N. (2002). 40Ar/39Ar geochronology and structural analysis: Basin evolution and detrital feedback mechanisms, Hold with Hope region, East Greenland. *Norsk Geologisk Tidsskrift*, 82(4), 341–358.
- Hayward, N., & Ebinger, C. (1996). Variations in the along-axis segmentation of the Afar Rift system. *Tectonics*, 15(2), 244–257. <https://doi.org/10.1029/95TC02292>
- Henriksen, N. (1985). The Caledonides of central East Greenland 70–76 N, The Caledonide orogen-Scandinavia and related areas, 1095–1113.
- Henriksen, N. (2003). Caledonian Orogen East Greenland 70–82 N. Geological map 1:100000, GEUS, Copenhagen, Denmark.
- Henstra, G. A., Grundvåg, S.-A., Johannessen, E. P., Kristensen, T. B., Midtkandal, I., Nystuen, J. P., et al. (2016). Depositional processes and stratigraphic architecture within a coarse-grained rift-margin turbidite system: The Wollaston Forland Group, East Greenland. *Marine and Petroleum Geology*, 76, 187–209. <https://doi.org/10.1016/j.marpetgeo.2016.05.018>
- Henstra, G. A., Rotevatn, A., Gawthorpe, R. L., & Ravnås, R. (2015). Evolution of a major segmented normal fault during multiphase rifting: The origin of plan-view zigzag geometry. *Journal of Structural Geology*, 74, 45–63. <https://doi.org/10.1016/j.jsg.2015.02.005>
- Higgins, A. K., Gilotti, J. A., & Smith, M. P. (Eds.) (2008). *The Greenland Caledonides. Evolution of the northeast margin of Laurentia* (368 pp.). CO: Boulder.
- Hower, J., Hurley, P., Pinson, W., & Fairbairn, H. (1963). The dependence of K-Ar age on the mineralogy of various particle size ranges in a shale. *Geochimica et Cosmochimica Acta*, 27(5), 405–410. [https://doi.org/10.1016/0016-7037\(63\)90080-2](https://doi.org/10.1016/0016-7037(63)90080-2)
- Jackson, C. A.-L., Bell, R. E., Rotevatn, A., & Tvedt, A. B. M. (2017). Techniques to determine the kinematics of syndimentary normal faults and implications for fault growth models. *Geological Society of London, Special Publications*, 439(1), 187–217. <https://doi.org/10.1144/SP439.22>
- Jackson, C. A. L., & Rotevatn, A. (2013). 3D seismic analysis of the structure and evolution of a salt-influenced normal fault zone: A test of competing fault growth models. *Journal of Structural Geology*, 54, 215–234. <https://doi.org/10.1016/j.jsg.2013.06.012>
- Jennings, S., & Thompson, G. R. (1986). Diagenesis of Plio-Pleistocene sediments of the Colorado River delta, southern California. *Journal of Sedimentary Research*, 56(1), 89–98.
- Johnson, C., & Gallagher, K. (2000). A preliminary Mesozoic and Cenozoic denudation history of the North East Greenland onshore margin. *Global and Planetary Change*, 24(3–4), 261–274. [https://doi.org/10.1016/S0921-8181\(00\)00012-6](https://doi.org/10.1016/S0921-8181(00)00012-6)
- Kalsbeek, F., Nutman, A. P., & Taylor, P. N. (1993). Palaeoproterozoic basement province in the Caledonian fold belt of North-East Greenland. *Precambrian Research*, 63(1–2), 163–178. [https://doi.org/10.1016/0301-9268\(93\)90010-Y](https://doi.org/10.1016/0301-9268(93)90010-Y)
- Keep, M., & McClay, K. (1997). Analogue modelling of multiphase rift systems. *Tectonophysics*, 273(3–4), 239–270. [https://doi.org/10.1016/S0040-1951\(96\)00272-7](https://doi.org/10.1016/S0040-1951(96)00272-7)
- Kelley, S. (2002). Excess argon in K-Ar and Ar-Ar geochronology. *Chemical Geology*, 188(1–2), 1–22. [https://doi.org/10.1016/S0009-2541\(02\)00064-5](https://doi.org/10.1016/S0009-2541(02)00064-5)
- Khalil, S. M., & McClay, K. R. (2001). Tectonic evolution of the NW Red Sea-Gulf of Suez rift system. *Geological Society of London, Special Publications*, 187(1), 453–473. <https://doi.org/10.1144/GSL.SP.2001.187.01.22>
- Kristensen, T. B., Rotevatn, A., Peacock, D. C. P., Henstra, G. A., Midtkandal, I., & Grundvåg, S.-A. (2016). Structure and flow properties of syn-rift border faults: The interplay between fault damage and fault-related chemical alteration (Dombjerg Fault, Wollaston Forland, NE Greenland). *Journal of Structural Geology*, 92, 99–115. <https://doi.org/10.1016/j.jsg.2016.09.012>
- Ksienzyk, A. K., Wemmer, K., Jacobs, J., Fossen, H., Schomberg, A. C., Süssenberger, A., et al. (2016). Post-Caledonian brittle deformation in the Bergen area, West Norway: Results from K-Ar illite fault gouge dating. *Norwegian Journal of Geology*, 96(3).
- Kübler, B. (1964). Les argiles, indicateurs de métamorphisme. *Revue. Institut Français du Pétrole*, 19, 1093–1112.
- Kübler, B. (1967). La cristallinité de l'illite et les zones tout-à-fait supérieures du métamorphisme. In J. P. Schaer (Ed.), *Colloque sur les étages tectoniques, à la Baconnière, Neuchâtel* (pp. 105–122). Neuchatel: Université Neuchatel a la Baconnière.
- Larsen, L. M., & Watt, W. S. (1985). Episodic volcanism during break-up of the North Atlantic: Evidence from the East Greenland plateau basalts. *Earth and Planetary Science Letters*, 73(1), 105–116. [https://doi.org/10.1016/0012-821X\(85\)90038-X](https://doi.org/10.1016/0012-821X(85)90038-X)
- Larsen, P. H. (1988). Relay structures in a lower Permian basement involved extension system, East Greenland. *Journal of Structural Geology*, 10(1), 3–8. [https://doi.org/10.1016/0191-8141\(88\)90122-8](https://doi.org/10.1016/0191-8141(88)90122-8)
- Larsen, P. H., & Bengaard, H. J. (1991). Devonian basin initiation in East Greenland: A result of sinistral wrench faulting and Caledonian extensional collapse. *Journal of the Geological Society*, 148(2), 355–368. <https://doi.org/10.1144/gsjgs.148.2.0355>
- Larsen, P.-H., Olsen, H., & Clack, J. A. (2008). The Devonian basin in East Greenland—Review of basin evolution and vertebrate assemblages. *Geological Society of America Memoirs*, 202, 273–292.
- Löbens, S., Bense, F. A., Wemmer, K., Dunkl, I., Costa, C. H., Layer, P., & Siegesmund, S. (2011). Exhumation and uplift of the Sierras Pampeanas: Preliminary implications from K-Ar fault gouge dating and low-T thermochronology in the Sierra de Comechingones (Argentina). *International Journal of Earth Sciences*, 100(2–3), 671–694. <https://doi.org/10.1007/s00531-010-0608-0>
- Lyons, J. B., & Snellenburg, J. (1971). Dating faults. *Geological Society of America Bulletin*, 82(6), 1749–1752. [https://doi.org/10.1130/0016-7606\(1971\)82%5B1749:DF%5D2.0.CO;2](https://doi.org/10.1130/0016-7606(1971)82%5B1749:DF%5D2.0.CO;2)
- Mats, V. D., & Perepelova, T. I. (2011). A new perspective on evolution of the Baikal Rift. *Geoscience Frontiers*, 2(3), 349–365. <https://doi.org/10.1016/j.gsf.2011.06.002>
- Maync, W. (1949). The cretaceous beds between Kuhn Island and Cape Franklin (Gauss Peninsula), northern East Greenland. *Meddelelser om Grønland*, 133(3), 1–291.
- Merriman, R., & Frey, M. (1999). Patterns of very low-grade metamorphism in metapelitic rocks. In M. Frey & D. Robertson (Eds.), *Low-grade metamorphism* (pp. 61–107). Oxford: Blackwell Science.
- Michon, L., & Sokoutis, D. (2005). Interaction between structural inheritance and extension direction during graben and depocentre formation: An experimental approach. *Tectonophysics*, 409(1–4), 125–146. <https://doi.org/10.1016/j.tecto.2005.08.020>
- Milani, E. J., & Davison, I. (1988). Basement control and transfer tectonics in the Recôncavo-Tucano-Jatobá rift, Northeast Brazil. *Tectonophysics*, 154(1–2), 41–70. [https://doi.org/10.1016/0040-1951\(88\)90227-2](https://doi.org/10.1016/0040-1951(88)90227-2)
- Miller, J. M., Norvick, M. S., & Wilson, C. J. L. (2002). Basement controls on rifting and the associated formation of ocean transform faults—Cretaceous continental extension of the southern margin of Australia. *Tectonophysics*, 359(1–2), 131–155. [https://doi.org/10.1016/S0040-1951\(02\)00508-5](https://doi.org/10.1016/S0040-1951(02)00508-5)
- Mjelde, R., Breivik, A., Raum, T., Mittelstaedt, E., Ito, G., & Faleide, J. (2008). Magmatic and tectonic evolution of the North Atlantic. *Journal of the Geological Society*, 165(1), 31–42. <https://doi.org/10.1144/0016-76492007-018>
- Morley, C., Nelson, R., Patton, T., & Munn, S. (1990). Transfer zones in the East African rift system and their relevance to hydrocarbon exploration in rifts (1). *AAPG Bulletin*, 74(8), 1234–1253.

- Moustafa, A. R. (1997). Controls on the development and evolution of transfer zones: The influence of basement structure and sedimentary thickness in the Suez rift and Red Sea. *Journal of Structural Geology*, 19(6), 755–768. [https://doi.org/10.1016/S0191-8141\(97\)00007-2](https://doi.org/10.1016/S0191-8141(97)00007-2)
- Müller, R., Petter Ngstuen, J., Eide, F., & Lie, H. (2005). Late Permian to Triassic basin infill history and palaeogeography of the mid-Norwegian shelf-East Greenland region. *Norwegian Petroleum Society Special Publications*, 12, 165–169.
- Nicol, A., Childs, C., Walsh, J. J., Manzocchi, T., & Schöpfer, M. P. J. (2017). Interactions and growth of faults in an outcrop-scale system. *Geological Society of London, Special Publications*, 439(1), 23–39.
- Nicol, A., Walsh, J., Berryman, K., & Nodder, S. (2005). Growth of a normal fault by the accumulation of slip over millions of years. *Journal of Structural Geology*, 27(2), 327–342. <https://doi.org/10.1016/j.jsg.2004.09.002>
- Nixon, C. W., McNeill, L. C., Bull, J. M., Bell, R. E., Gawthorpe, R. L., Henstock, T. J., et al. (2016). Rapid spatiotemporal variations in rift structure during development of the Corinth Rift, Central Greece. *Tectonics*, 35, 1225–1248. <https://doi.org/10.1002/2015TC004026>
- Odinsen, T., Christiansson, P., Gabrielsen, R. H., Faleide, J. I., & Berge, A. M. (2000). The geometries and deep structure of the northern North Sea rift system. *Geological Society of London, Special Publications*, 167(1), 41–57. <https://doi.org/10.1144/GSL.SP.2000.167.01.03>
- Osmundsen, P. T., Sommaruga, A., Skilbrei, J. R., & Olesen, O. (2002). Deep structure of the mid Norway rifted margin. *Norwegian Journal of Geology*, 82, 205–224.
- Peacock, D. C. P., Price, S. P., & Pickles, C. S. (2000). The world's biggest relay ramp: Hold with hope, NE Greenland. *Journal of Structural Geology*, 22(7), 843–850. [https://doi.org/10.1016/S0191-8141\(00\)00012-2](https://doi.org/10.1016/S0191-8141(00)00012-2)
- Phillips, T. B., Jackson, C. A. L., Bell, R. E., Duffy, O. B., & Fossen, H. (2016). Reactivation of intrabasement structures during rifting: A case study from offshore southern Norway. *Journal of Structural Geology*, 91, 54–73. <https://doi.org/10.1016/j.jsg.2016.08.008>
- Pleuger, J., Mancktelow, N., Zwingmann, H., & Manser, M. (2012). K-Ar dating of synkinematic clay gouges from Nealpine faults of the central, western and eastern alps. *Tectonophysics*, 550, 1–16.
- Price, S., Brodie, J., Whitham, A., & Kent, R. (1997). Mid-Tertiary rifting and magmatism in the Trill Ø region, East Greenland. *Journal of the Geological Society*, 154(3), 419–434. <https://doi.org/10.1144/gsjgs.154.3.0419>
- Rotevatn, A., Jackson, C. A. L., Tvedt, A. B. M., Bell, R. E., & Blækkam, I. (2018). How do normal faults grow?, Preprint retrieved from [eartharxiv.org/r9hf](https://arxiv.org/abs/1809.09191).
- Salomon, E., Koehn, D., & Passchier, C. (2015). Brittle reactivation of ductile shear zones in NW Namibia in relation to South Atlantic rifting. *Tectonics*, 34, 70–85. <https://doi.org/10.1002/2014TC003728>
- Seidler, L., Steel, R., Stemmerik, L., & Surlyk, F. (2004). North Atlantic marine rifting in the Early Triassic: New evidence from East Greenland. *Journal of the Geological Society*, 161(4), 583–592. <https://doi.org/10.1144/0016-764903-063>
- Smith, M., & Mosley, P. (1993). Crustal heterogeneity and basement influence on the development of the Kenya Rift, East Africa. *Tectonics*, 12(2), 591–606. <https://doi.org/10.1029/92TC01710>
- Solum, J. G., van der Pluijm, B. A., & Peacor, D. R. (2005). Neocrystallization, fabrics and age of clay minerals from an exposure of the Moab Fault, Utah. *Journal of Structural Geology*, 27(9), 1563–1576. <https://doi.org/10.1016/j.jsg.2005.05.002>
- Srodon, J., & Eberl, D. D. (1984). Illite. *Reviews in Mineralogy and Geochemistry*, 13(1), 495–544.
- Steel, R., & Ryseth, A. (1990). The Triassic-Early Jurassic succession in the northern North Sea: Megasequence stratigraphy and intra-Triassic tectonics. *Geological Society of London, Special Publications*, 55(1), 139–168. <https://doi.org/10.1144/GSL.SP.1990.055.01.07>
- Stemmerik, L., Vigran, J. O., & Piasecki, S. (1991). Dating of Late Paleozoic rifting events in the North Atlantic: New biostratigraphic data from the uppermost Devonian and Carboniferous of East Greenland. *Geology*, 19(3), 218–221. [https://doi.org/10.1130/0091-7613\(1991\)019%3C0218:DOLPRE%3E2.3.CO;2](https://doi.org/10.1130/0091-7613(1991)019%3C0218:DOLPRE%3E2.3.CO;2)
- Strachan, R., Friderichsen, J., Holdsworth, R., & Jepsen, H. (1994). Regional geology and Caledonian structure, Dronning Louise Land, North-East Greenland. *Geology of North-East Greenland. Rapport Grønlands Geologiske Undersøgelse*, 162, 71–76.
- Strachan, R., Nutman, A., & Friderichsen, J. (1995). SHRIMP U-Pb geochronology and metamorphic history of the Smaldefjord sequence, NE Greenland Caledonides. *Journal of the Geological Society*, 152(5), 779–784. <https://doi.org/10.1144/gsjgs.152.5.0779>
- Strachan, R. A. (1994). Evidence in North-East Greenland for Late Silurian-Early Devonian regional extension during the Caledonian orogeny. *Geology*, 22(10), 913–916. [https://doi.org/10.1130/0091-7613\(1994\)022%3C0913:EINEGF%3E2.3.CO;2](https://doi.org/10.1130/0091-7613(1994)022%3C0913:EINEGF%3E2.3.CO;2)
- Surlyk, F. (1978). Submarine fan sedimentation along fault scarps on tilted fault blocks. *Bulletin Grønlands Geologiske Undersøgelse*, 128, 1–128.
- Surlyk, F. (1984). Fan-delta to submarine fan conglomerates of the Volgian-Valanginian Wollaston Forland Group, East Greenland.
- Surlyk, F. (1990). Timing, style and sedimentary evolution of Late Palaeozoic-Mesozoic extensional basins of East Greenland. *Geological Society of London, Special Publications*, 55(1), 107–125. <https://doi.org/10.1144/GSL.SP.1990.055.01.05>
- Surlyk, F. (1991). Sequence stratigraphy of the Jurassic-lowermost Cretaceous of East Greenland (1). *AAPG Bulletin*, 75(9), 1468–1488.
- Surlyk, F. (2003). The Jurassic of East Greenland: A sedimentary record of thermal subsidence, onset and culmination of rifting. *Geological Survey of Denmark Greenland Bulletin*, 1, 659–722.
- Surlyk, F., Clemmensen, L. B., & Larsen, H. (1981). Post-Paleozoic evolution of the East Greenland continental margin.
- Surlyk, F., Hurst, J., Piasecki, S., Rolle, F., Scholle, P., Stemmerik, L., & Thomsen, E. (1986). The Permian of the western margin of the Greenland Sea—A future exploration target.
- Surlyk, F., & Korstgård, J. (2013). Crestal unconformities on an exposed Jurassic tilted fault block, Wollaston Forland, East Greenland as an analogue for buried hydrocarbon traps. *Marine and Petroleum Geology*, 44, 82–95. <https://doi.org/10.1016/j.marpetgeo.2013.03.009>
- Surlyk, F., Piasecki, S., Rolle, F., Stemmerik, L., Thomsen, E., & Wrang, P. (1984). The Permian base of east Greenland. In *Petroleum geology of the North European margin* (pp. 303–315). Dordrecht: Springer.
- Tenthorey, E., Cox, S. F., & Todd, H. F. (2003). Evolution of strength recovery and permeability during fluid-rock reaction in experimental fault zones. *Earth and Planetary Science Letters*, 206(1–2), 161–172. [https://doi.org/10.1016/S0012-821X\(02\)01082-8](https://doi.org/10.1016/S0012-821X(02)01082-8)
- Theunissen, K., Klerck, J., Melnikov, A., & Mruma, A. (1996). Mechanisms of inheritance of rift faulting in the western branch of the East African Rift, Tanzania. *Tectonics*, 15(4), 776–790. <https://doi.org/10.1029/95TC03685>
- Tomasso, M., Underhill, J. R., Hodgkinson, R. A., & Young, M. J. (2008). Structural styles and depositional architecture in the Triassic of the Ninian and Alwyn north fields: Implications for basin development and prospectivity in the northern North Sea. *Marine and Petroleum Geology*, 25(7), 588–605. <https://doi.org/10.1016/j.marpetgeo.2007.11.007>
- Tommasi, A., & Vauchez, A. (2001). Continental rifting parallel to ancient collisional belts: An effect of the mechanical anisotropy of the lithospheric mantle. *Earth and Planetary Science Letters*, 185(1–2), 199–210. [https://doi.org/10.1016/S0012-821X\(00\)00350-2](https://doi.org/10.1016/S0012-821X(00)00350-2)
- Torgersen, E., Viola, G., Zwingmann, H., & Harris, C. (2014). Structural and temporal evolution of a reactivated brittle-ductile fault—Part II: Timing of fault initiation and reactivation by K-Ar dating of synkinematic illite/muscovite. *Earth and Planetary Science Letters*, 407, 221–233. <https://doi.org/10.1016/j.epsl.2014.09.031>
- Torsvik, T., Smethurst, M., Meert, J. G., Van der Voo, R., McKerrow, W., Brasier, M., et al. (1996). Continental break-up and collision in the Neoproterozoic and Palaeozoic—A tale of Baltica and Laurentia. *Earth-Science Reviews*, 40(3–4), 229–258. [https://doi.org/10.1016/0012-8252\(96\)00008-6](https://doi.org/10.1016/0012-8252(96)00008-6)

- Tvedt, A. B. M., Rotevatn, A., & Jackson, C. A. L. (2016). Supra-salt normal fault growth during the rise and fall of a diapir: Perspectives from 3D seismic reflection data, Norwegian North Sea. *Journal of Structural Geology*, *91*, 1–26.
- van der Pluijm, B. A., Hall, C. M., Vrolijk, P. J., Pevear, D. R., & Covey, M. C. (2001). The dating of shallow faults in the Earth's crust. *Nature*, *412*(6843), 172–175. <https://doi.org/10.1038/35084053>
- Vauchez, A., Barruol, G., & Tommasi, A. (1997). Why do continents break-up parallel to ancient orogenic belts? *Terra Nova*, *9*(2), 62–66. <https://doi.org/10.1111/j.1365-3121.1997.tb00003.x>
- Viola, G., Scheiber, T., Fredin, O., Zwingmann, H., Margreth, A., & Knies, J. (2016). Deconvoluting complex structural histories archived in brittle fault zones. *Nature Communications*, *7*, 13448. <https://doi.org/10.1038/ncomms13448>
- Vischer, A. (1943). Die postdevonische Tektonik von Ostgrönland zwischen 74° und 75° N. Br., Kuhn Ø, Wollaston Forland, Clavering Ø und angrenzende Gebiete. *Meddelelser om Grønland*, *133*(1), 1–195.
- Vrolijk, P., & van der Pluijm, B. A. (1999). Clay gouge. *Journal of Structural Geology*, *21*(8–9), 1039–1048. [https://doi.org/10.1016/S0191-8141\(99\)00103-0](https://doi.org/10.1016/S0191-8141(99)00103-0)
- Walsh, J. J., Bailey, W. R., Childs, C., Nicol, A., & Bonson, C. G. (2003). Formation of segmented normal faults: A 3-D perspective. *Journal of Structural Geology*, *25*(8), 1251–1262. [https://doi.org/10.1016/S0191-8141\(02\)00161-X](https://doi.org/10.1016/S0191-8141(02)00161-X)
- Walsh, J. J., Nicol, A., & Childs, C. (2002). An alternative model for the growth of faults. *Journal of Structural Geology*, *24*(11), 1669–1675. [https://doi.org/10.1016/S0191-8141\(01\)00165-1](https://doi.org/10.1016/S0191-8141(01)00165-1)
- Whipp, P., Jackson, C., Gawthorpe, R., Dreyer, T., & Quinn, D. (2014). Normal fault array evolution above a reactivated rift fabric; a subsurface example from the northern Horda Platform, Norwegian North Sea. *Basin Research*, *26*(4), 523–549. <https://doi.org/10.1111/bre.12050>
- White, A. P., & Hodges, K. V. (2003). Pressure-temperature-time evolution of the Central East Greenland Caledonides: Quantitative constraints on crustal thickening and synorogenic extension. *Journal of Metamorphic Geology*, *21*(9), 875–897. <https://doi.org/10.1046/j.1525-1314.2003.00489.x>
- White, A. P., Hodges, K. V., Martin, M. W., & Andresen, A. (2002). Geologic constraints on middle-crustal behavior during broadly synorogenic extension in the central East Greenland Caledonides. *International Journal of Earth Sciences*, *91*(2), 187–208. <https://doi.org/10.1007/s005310100227>
- Whitham, A., Price, S., Koraini, A., & Kelly, S. (1999). *Cretaceous (post-Valanginian) sedimentation and rift events in NE Greenland (71–77 N)*. Paper presented at Geological Society, London, Petroleum Geology Conference series, Geological Society of London.
- Worthington, R. P., & Walsh, J. J. (2011). Structure of lower Carboniferous basins of NW Ireland, and its implications for structural inheritance and Cenozoic faulting. *Journal of Structural Geology*, *33*(8), 1285–1299. <https://doi.org/10.1016/j.jsg.2011.05.001>
- Yan, Y., van der Pluijm, B. A., & Peacor, D. R. (2001). Deformation microfabrics of clay gouge, Lewis thrust, Canada: A case for fault weakening from clay transformation. *Geological Society of London, Special Publications*, *186*(1), 103–112. <https://doi.org/10.1144/GSL.SP.2001.186.01.07>
- Younes, A. I., & McClay, K. (2002). Development of accommodation zones in the Gulf of Suez-Red Sea rift, Egypt. *AAPG Bulletin*, *86*(6), 1003–1026.
- Zwingmann, H., & Mancktelow, N. (2004). Timing of Alpine fault gouges. *Earth and Planetary Science Letters*, *223*(3–4), 415–425. <https://doi.org/10.1016/j.epsl.2004.04.041>
- Zwingmann, H., Mancktelow, N., Antognini, M., & Lucchini, R. (2010). Dating of shallow faults: New constraints from the AlpTransit tunnel site (Switzerland). *Geology*, *38*(6), 487–490. <https://doi.org/10.1130/G30785.1>